

Supplementary Information
for
Titanium-mediated coupling of CO₂ and ethylene to acrylate: mechanistic insights from Cp*₂Ti complexes

Areum Kim,^a Nayeong Seok,^b Mijung Lee,^c Young Kyu Hwang,^c Jeongcheol Shin^{d*} and
Changho Yoo^{a,b*}

^aDepartment of Chemistry, Ulsan National Institute of Science and Technology (UNIST),
Ulsan 44919, Republic of Korea

^bGraduate School of Carbon Neutrality, Ulsan National Institute of Science and Technology
(UNIST), Ulsan 44919, Republic of Korea

^cGreen Carbon Catalysis Research Center, Korea Research Institute of Chemical
Technology (KRICT), Daejeon 34114, Republic of Korea

^dDepartment of Chemistry, Duksung Women's University, Seoul 01369, Republic of Korea

*Corresponding Author E-mail Address: cyoo@unist.ac.kr, jcshin91@duksung.ac.kr

Table of Contents	S2
I. Synthesis and Characterization of Compounds	S3
II. NMR Spectra	S8
III. EPR Spectra	S10
IV. UV-Vis Spectra	S12
V. IR Spectra	S13
VI. Kinetic Studies on Formation of 2	S14
VII. Formation of 2 with Varying C₂H₄ and CO₂ Equivalents	S16
VIII. Conversion of 5 to Methyl Acrylate and PMA	S18
IX. Deprotonation of 2	S22
X. Catalytic Acrylate Synthesis	S26
XI. Crystallographic Details	S27
XII. Cyclic Voltammograms	S32
XIII. DFT Calculation	S35
XIV. Reference	S59

I. Synthesis and Characterization of Compounds

General Considerations. All manipulations were carried out using standard Schlenk or glovebox techniques under a N₂ atmosphere. Solvents were degassed and dried by passage through an activated alumina, and stored over 4 Å molecular sieves. Compounds **1** and Cp*₂Ti(OTf) were prepared according to the literature procedures.^{1,2} Ethylene (99.99%) and CO₂ gas (purity: 99.999%) were purchased and used without any further purification. All other reagents were purchased from commercial vendors and used without further purification unless otherwise stated. Elemental Analyses were carried out at UNIST Office of Research Facilities and Training on Thermo Scientific FLASH 2000 series.

Spectroscopic Measurements. ¹H and ¹³C{¹H} NMR spectra were recorded on Bruker Advance 400 and 600 MHz spectrometers at 298 K. NMR solvents were purchased from Deutero and Sigma Aldrich. Benzene-*d*₆ (C₆D₆), chloroform-*d* (CDCl₃), acetonitrile-*d*₃ (CD₃CN), toluene-*d*₈ and tetrahydrofuran-*d*₈ were freeze-pump-thaw degassed three times before drying by passage through a small column of activated alumina and storage over 4 Å molecular sieves. Deuterium oxide (D₂O) was used without further purification. ¹H and ¹³C{¹H} NMR chemical shifts are reported in ppm relative to residual solvent resonances. Solution magnetic moments were determined by the Evans method.³ The CW X-band EPR spectra were collected on a Bruker EMXplus spectrometer. EPR spectra of Ti^{III} complexes were dissolved in a catalytically relevant THF solvent and measured at 298 K. The resulting EPR spectra were simulated with Easyspin software package.⁴ Infrared (IR) spectra were recorded in KBr pellet by a Thermo Scientific Nicolet iS10 FTIR. UV-Vis spectra were measured by a JASCO V-670 UV-Vis spectrophotometer

using a 1 cm two-window quartz spectrophotometer cell sealed with a screw-cap purchased from Hellma Analytics (117.104-QS).

Synthesis of Cp*₂Ti(C₂H₄) (1). Compound **1** was prepared following literature procedures with minor modification.¹ To a solution of Cp*₂TiCl₂ (1.000 g, 2.569 mmol) in 30 mL toluene in 100 mL Schlenk flask was added a n-BuLi (2.26 mL, 2.5M in hexane, 5.65 mmol) at -78 °C, and the reaction mixture was stirred for 1 h at same temperature. The mixture was degassed by freeze-pump-thaw cycles on the Schlenk line and C₂H₄ was charged under ambient conditions. The reaction mixture was stirred at room temperature for 48 h resulting in a color change from red to dark brownish-green. The volatiles were removed under vacuum, and the residue was dissolved with pentane and filtered through a short plug of Celite. The filtrate was dried under vacuum and the resulting powder was recrystallized from pentane at -35 °C to give **1** as a green powder (449 mg, 1.296 mmol, 50%). Spectroscopic data were in good agreement with those previously reported.⁵ **¹H NMR** (400 MHz, C₆D₆) δ 2.07 (s, 4H, C₂H₄), δ 1.69 (s, 30H, Cp*-CH₃). **¹³C NMR** (101 MHz, C₆D₆) δ 119.76 (Cp*-C), δ 105.03 (C₂H₄), δ 11.88 (Cp*-CH₃). **IR** (KBr pellet, cm⁻¹): ν_{Ar} 1435, 1381, ν_{C₂H₄} 1075. **UV-Vis** [THF, nm (L mol⁻¹ cm⁻¹): 280 (19800), 922 (32). Crystals suitable for X-ray diffraction were grown by layering a saturated THF solution of **1** with diethyl ether at -35 °C.

Synthesis of Cp*₂Ti(C₂H₄CO₂) (2). A solution of Cp*₂Ti(C₂H₄) (**1**, 300 mg, 0.866 mmol) in 20 mL toluene in 100 mL Schlenk flask was degassed by freeze-pump-thaw cycles on the Schlenk line. CO₂ was charged under ambient conditions resulting in an immediate color change from green to red. The solution was stirred for 30 min at room temperature, and all volatiles were removed under vacuum. The resulting solid was washed with pentane, dissolved in benzene and filtered

through a short plug of Celite. The resulting product **2** (287 mg, 0.735 mmol, 85%) was isolated as an orange powder after drying under vacuum. Spectroscopic data were in good agreement with those previously reported.⁶ **¹H NMR** (400 MHz, C₆D₆) δ 3.41 (t, *J* = 8.0 Hz, 2H, CH₂CH₂CO₂), δ 1.67 (s, 30H, Cp*-CH₃), δ 1.14 (t, *J* = 8.0 Hz, 2H, CH₂CH₂CO₂). **¹³C NMR** (101 MHz, C₆D₆) δ 171.92 (CH₂CH₂CO₂), δ 124.08 (Cp*-C), δ 54.01 (CH₂CH₂CO₂), δ 53.61 (CH₂CH₂CO₂), δ 11.64 (10C, Cp*-CH₃). **IR** (KBr pellet, cm⁻¹): ν_{C=O} 1670, ν_{Ar} 1435, 1381. **UV-Vis** [THF, nm (L mol⁻¹ cm⁻¹): 260 (25800), ~420 (sh, 280). Crystals suitable for X-ray diffraction were grown by layering a saturated toluene solution of **2** with pentane at -35 °C.

Synthesis of [Cp*₂Ti(C₂H₄CO₂Me)][OTf] (5**).** To a solution of Cp*₂Ti(C₂H₄CO₂) (**2**, 100 mg, 0.256 mmol) in toluene 5 mL was added MeOTf (28.0 μL, 0.256 mmol) at -35 °C. The mixture was allowed to warm to ambient temperature and stirred for 2 h resulting in a color change from orange to reddish-brown. After volatiles were removed in vacuum, the residue was washed in benzene, dissolved in THF and filtered through Celite. The resulting product **5** (116 mg, 0.209 mmol, 83%) was isolated as a reddish-brown powder after drying under vacuum. **¹H NMR** (400 MHz, CDCl₃) δ 3.88 (s, 3H, OCH₃), δ 3.25 (t, *J* = 7.84 Hz, 2H, CH₂CH₂CO₂), δ 1.92 (s, 30H, Cp*-CH₃), δ 1.42 (t, *J* = 7.84 Hz, 2H, CH₂CH₂CO₂). **¹³C NMR** (101 MHz, CDCl₃) δ 182.22 (CH₂CH₂CO₂), δ 128.61 (Cp*-C), δ 120.93 (q, ¹J_{C-F} = 214 Hz, CF₃), δ 57.28 (OCH₃), δ 49.37 (CH₂CH₂CO₂), δ 42.12 (CH₂CH₂CO₂), δ 11.99 (Cp*-CH₃). **IR** (KBr pellet, cm⁻¹): ν_{C=O} 1612, ν_{Ar} 1435, 1381. **UV-Vis** [THF, nm (L mol⁻¹ cm⁻¹): 260 (30700), 453 (524), ~550 (sh, 330). **Anal. Calcd.** for C₂₅H₃₇F₃O₅STi: C, 54.15; H, 6.72. Found: C, 53.66; H, 6.79. Crystals suitable for X-ray diffraction were grown by layering a saturated THF solution of **5** with diethyl ether at -35 °C.

Synthesis of [Na(THF)₂][Cp*₂Ti(C₂H₄CO₂)] (6**).** Sodium (20 mg, 0.87 mmol) was added to the solution of naphthalene (66 mg, 0.51 mmol) in 3 mL THF and the reaction mixture was stirred

for 3 h at room temperature. The resulting sodium naphthalide solution was filtered away from remaining sodium and added dropwise to the orange solution of Cp*₂Ti(C₂H₄CO₂) (**2**, 200 mg, 0.512 mmol) in 20 mL THF at –35 °C resulting an immediate color change to greenish-brown. The reaction mixture was stirred for 10 min at room temperature, and the volatiles were removed under vacuum. The residue was washed sequentially with pentane and benzene. The remaining solid was dissolved in THF and filtered through Celite. The filtrate was dried under vacuum to give a green powder of **6** (143 mg, 0.257 mmol, 50%). μ_{eff} : 1.77 μB (tetrahydrofuran-*d*₈, 25 °C, Evans method). **EPR**: $g_{\text{iso}} = 1.983$, $A(\text{Ti}) = 26$ MHz, $A(2\text{H}) = 5.8$ MHz. **IR** (KBr pellet, cm⁻¹): $\nu_{\text{C=O}}$ 1540, ν_{Ar} 1435, 1381. **UV-Vis** [THF, nm (L mol⁻¹ cm⁻¹): 258 (47800), ~420 (sh, 3130), ~600 (sh, 11), 856 (16). **Anal. Calcd.** for C₃₁H₅₀NaO₄Ti: C, 66.78; H, 9.04. Found: C, 66.68; H, 8.71. Crystals suitable for X-ray diffraction were grown by layering a saturated THF solution of **6** with diethyl ether at –35 °C.

Synthesis of Cp*₂Ti(O₂CCH=CH₂) (7**).** Tetrabutylammonium acrylate was synthesized by mixing tetrabutylammonium hydroxide 30-hydrate and acrylic acid in 1:1 ratio in MeOH and drying under vacuum. The resulting tetrabutylammonium acrylate (32 mg, 0.102 mmol, 1.2 equiv) was added to a solution of Cp*₂Ti(OTf) (45 mg, 0.096 mmol) in 5 mL toluene, inducing an immediate color change from dark green to dark blue. After the reaction mixture was stirred for 5 h at room temperature, the volatiles were removed under vacuum. The residue was dissolved with pentane and filtered through glass fiber filter. The filtrate was dried under vacuum to give an indigo powder of **7** (36 mg, 0.092 mmol, 96%). μ_{eff} : 1.69 μB (C₆D₆, 25 °C, Evans method). **EPR**: $g_{\text{iso}} = 1.977$, $A(\text{Ti}) = 21$ MHz. **IR** (KBr pellet, cm⁻¹): $\nu_{\text{C=C}}$ 1638, ν_{CO_2} 1522. **UV-Vis** [THF, nm (L mol⁻¹ cm⁻¹): 233 (167000), ~275 (sh, 88000), 628 (65), 752 (50). **Anal. Calcd.** for C₂₃H₃₃O₂Ti: C,

70.95; H, 8.54. Found: C, 70.34; H, 8.60. Crystals suitable for X-ray diffraction were grown by layering a saturated toluene solution of **7** with pentane at $-35\text{ }^{\circ}\text{C}$.

II. NMR Spectra

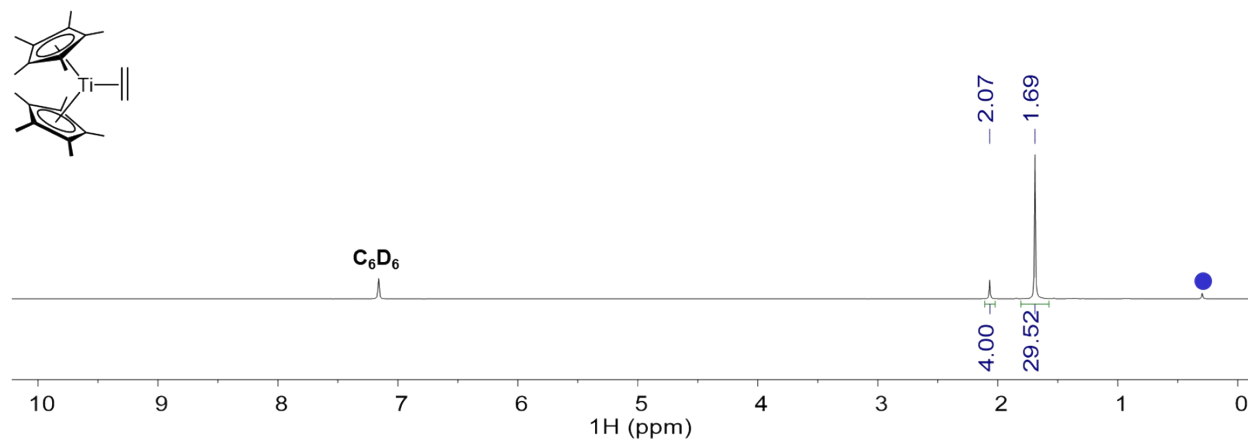


Figure S1. ^1H NMR spectrum of **1** (400MHz, C_6D_6) (●: grease).

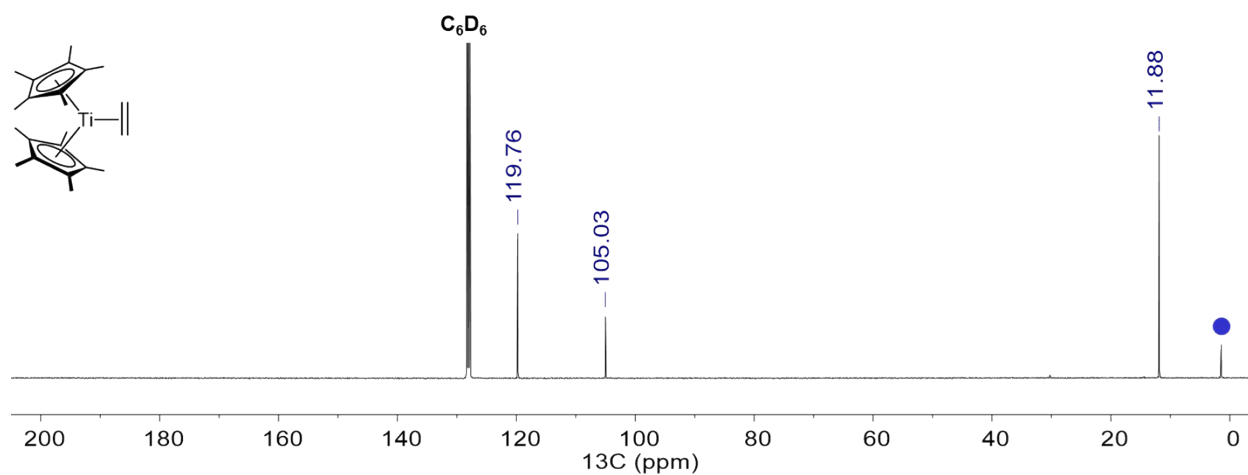


Figure S2. $^{13}\text{C}\{^1\text{H}\}$ NMR spectrum of **1** (101MHz, C_6D_6) (●: grease).

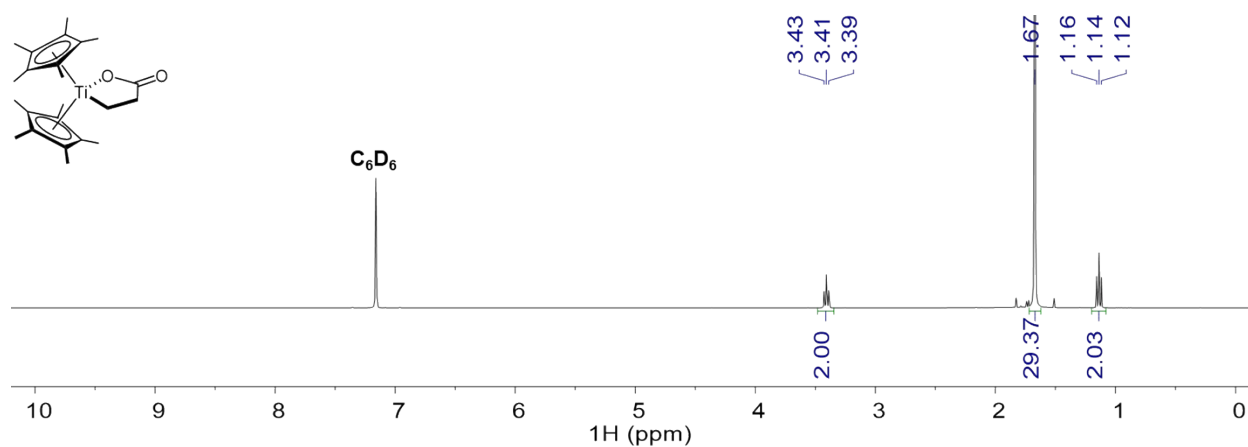


Figure S3. ^1H NMR spectrum of **2** (400MHz, C_6D_6)

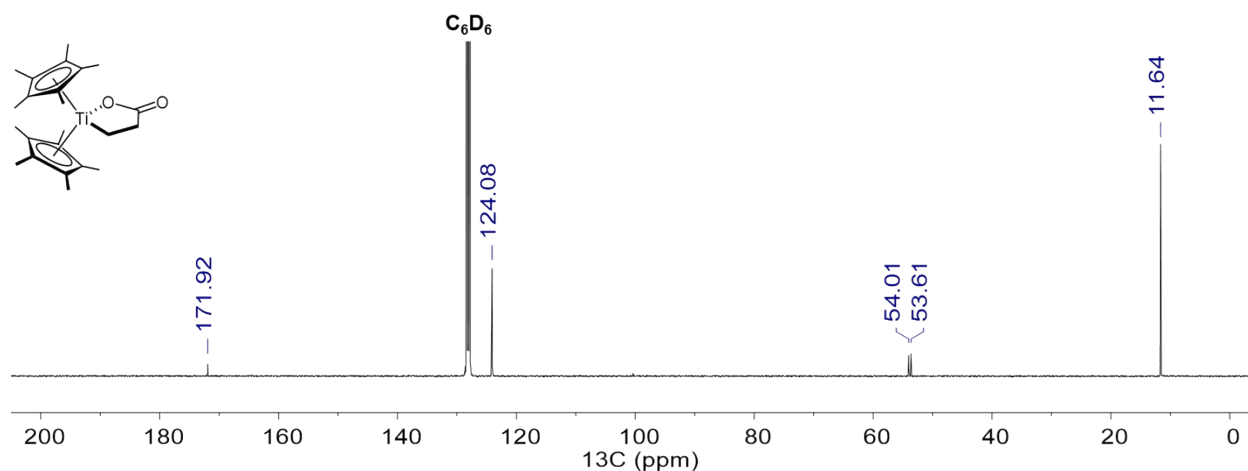


Figure S4. $^{13}\text{C}\{^1\text{H}\}$ NMR spectrum of **2** (101MHz, C_6D_6)

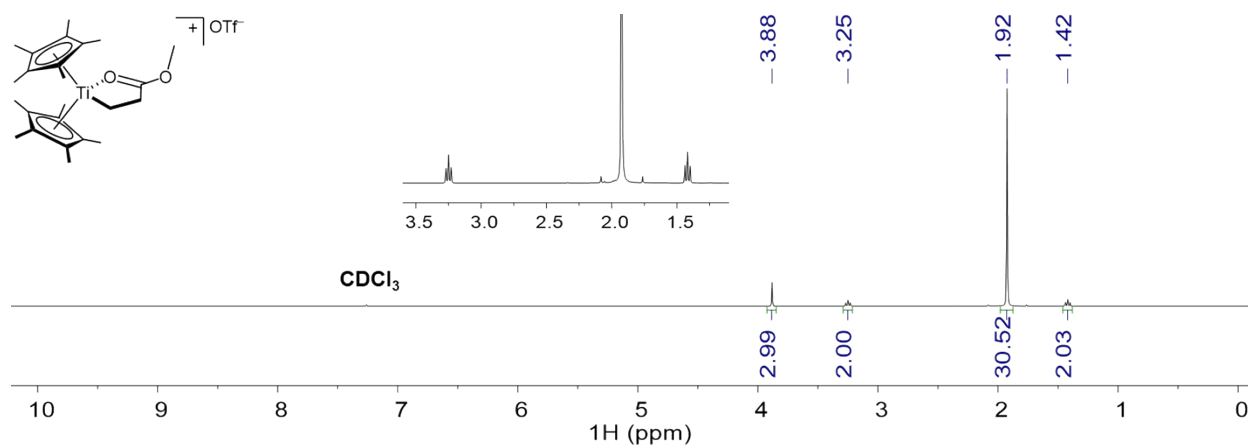


Figure S5. ^1H NMR spectrum of **5** (400MHz, CDCl_3)

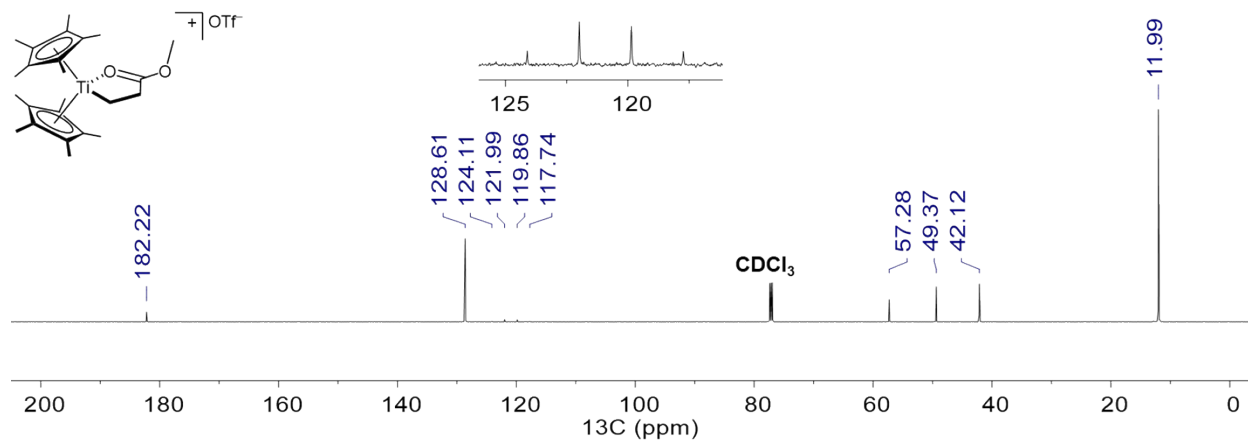


Figure S6. $^{13}\text{C}\{^1\text{H}\}$ NMR spectrum of **5** (101MHz, CDCl_3)

III. EPR Spectra

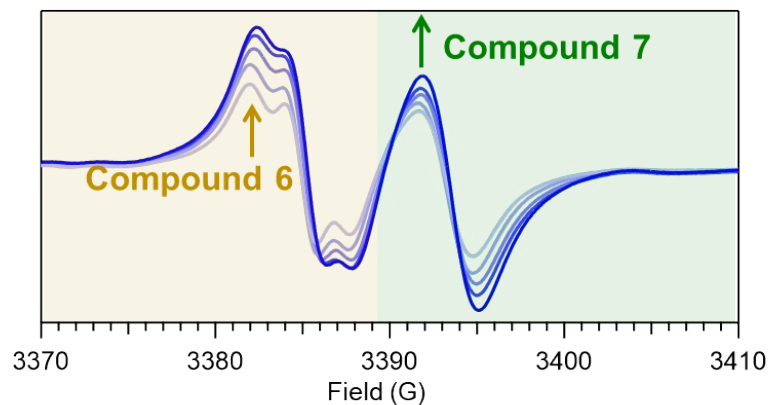


Figure S7. EPR spectroscopic reaction kinetics of NaO'Bu-assisted generation of Ti^{III} complexes **6** and **7** from **2**. Spectra were measured with the same parameter in THF at 298 K. The spectra were measured at 10, 30, 60, 210, and 720 minutes after the mixing of 10 equiv NaO'Bu to **2**.

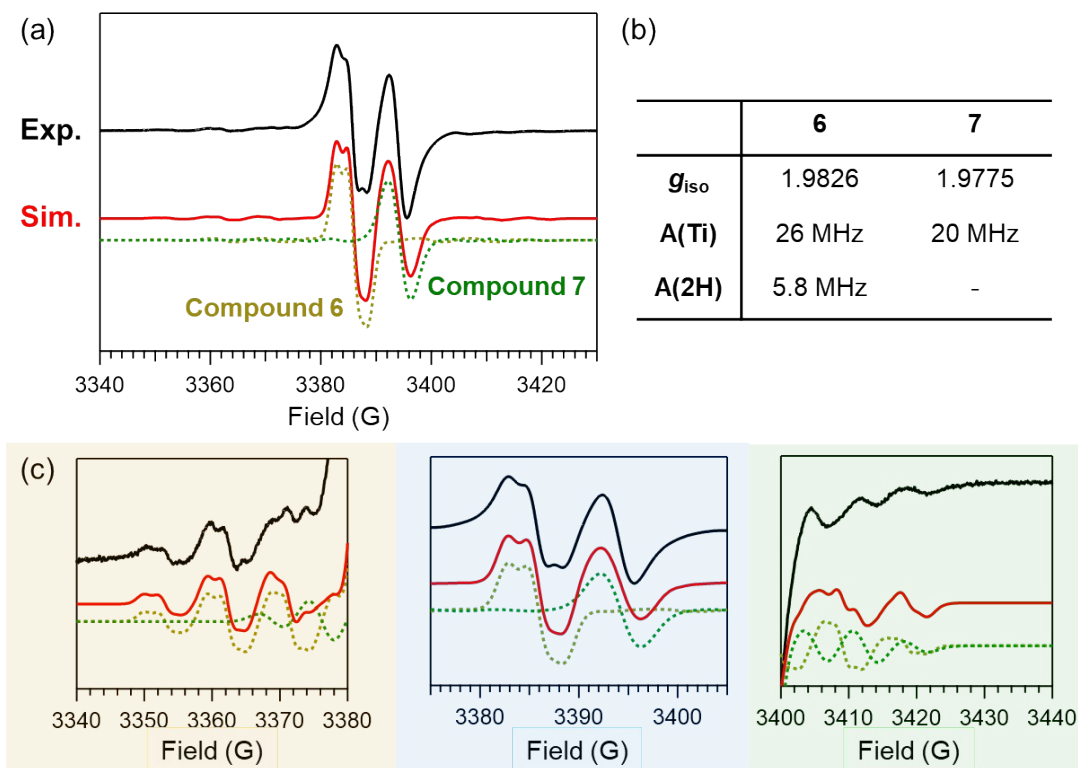


Figure S8. (a) Experimental (black) and simulated (red) EPR spectrum of two Ti^{III} complexes **6** and **7** generated by the addition of NaO'Bu to **2**. (b) The parameter used for the EPR simulation. (c) The expansion of various ranges. The experimental spectrum was collected with microwave frequency of 9.3946 GHz, microwave power of 0.01 mW, and modulation amplitude of 0.1 G at 298 K.

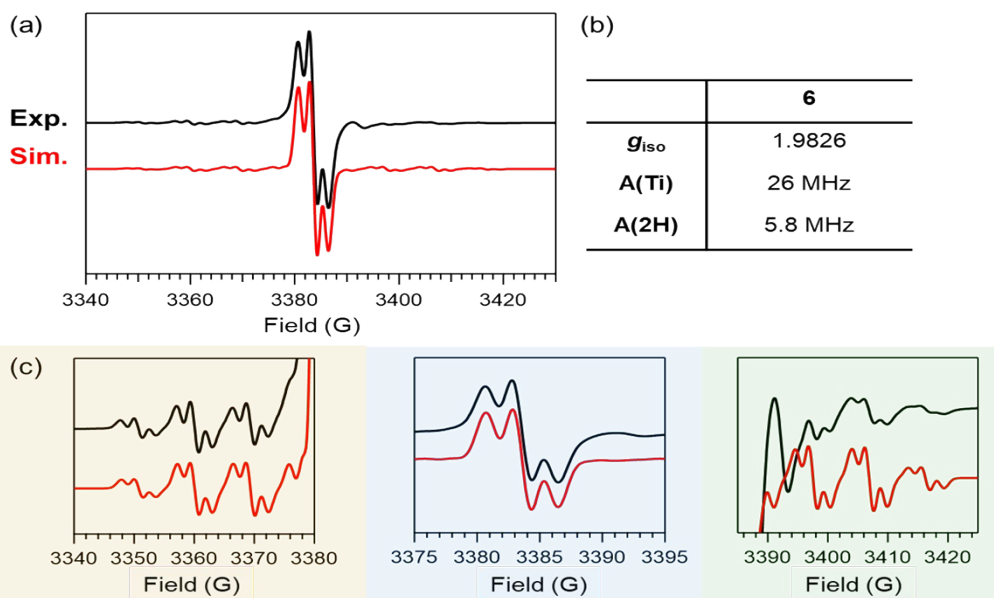


Figure S9. (a) Experimental (black) and simulated (red) X-band EPR spectrum of **6** measured in THF at 298 K. (b) The parameter used for the EPR simulation. (c) The expansion of various ranges. The experimental spectrum was collected with microwave frequency of 9.3890 GHz, microwave power of 1 mW, and modulation amplitude of 1 G at 298 K.

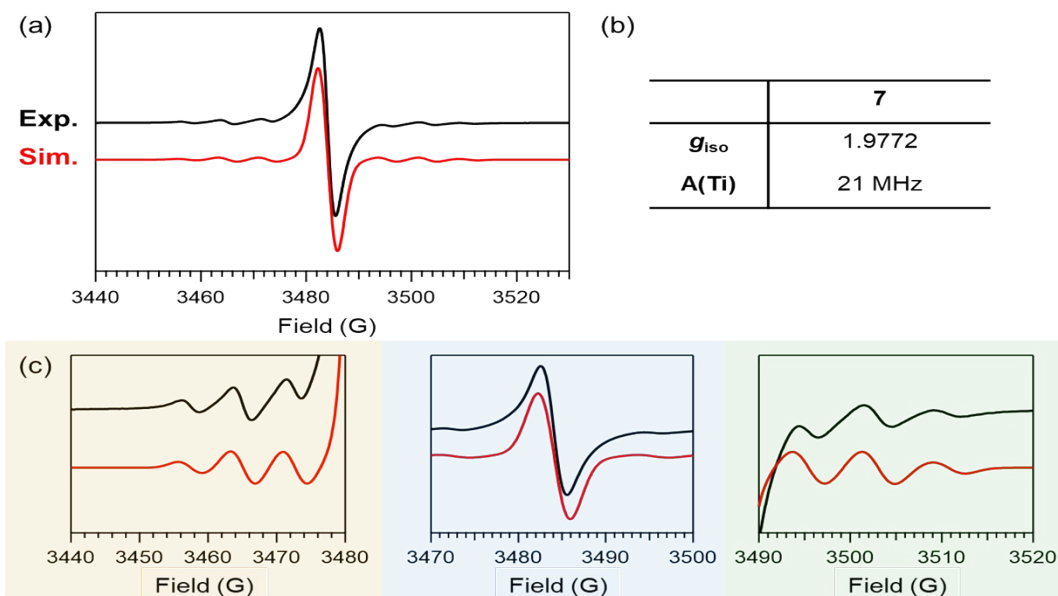


Figure S10. (a) Experimental (black) and simulated (red) X-band EPR spectrum of **7** measured at 298 K THF. (b) The parameter used for the EPR simulation. (c) The expansion of various ranges. The experimental spectrum was collected with microwave frequency of 9.6415 GHz, microwave power of 0.9 mW, and modulation amplitude of 0.5 G at 298 K.

IV. UV-Vis Spectra

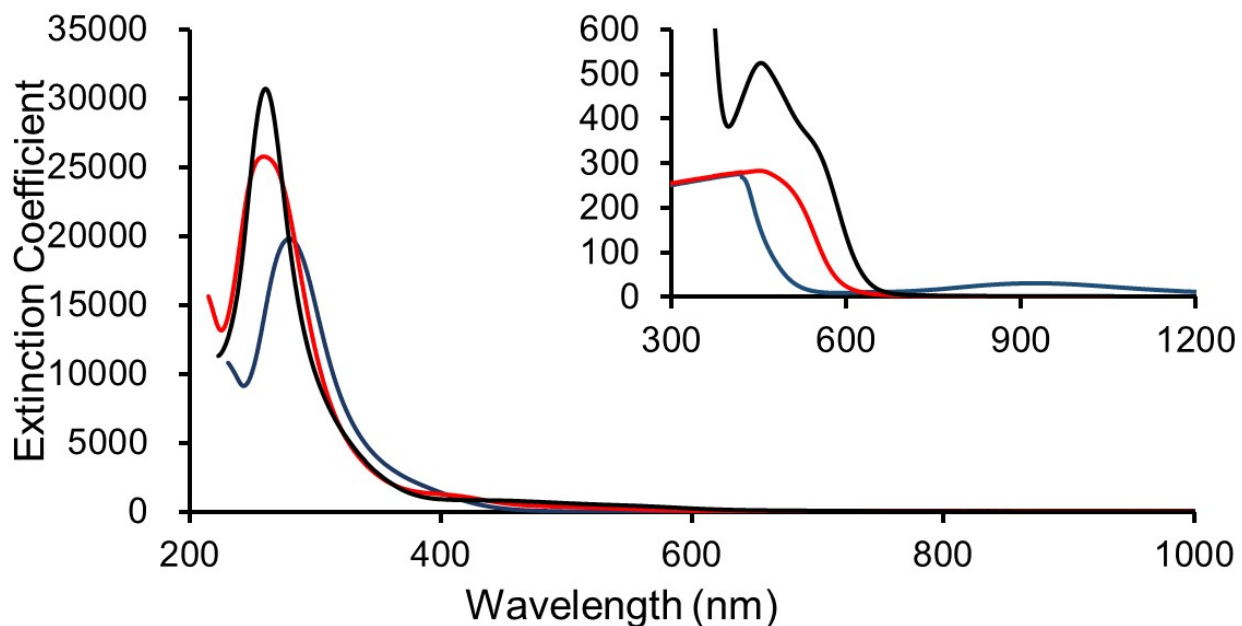


Figure S11. UV-Vis spectra of $\text{Cp}^*_2\text{Ti}(\text{C}_2\text{H}_4)$ (**1**, blue line), $\text{Cp}^*_2\text{Ti}(\text{C}_2\text{H}_4\text{CO}_2)$ (**2**, red line), $[\text{Cp}^*_2\text{Ti}(\text{C}_2\text{H}_4\text{CO}_2\text{Me})][\text{OTf}]$ (**5**, black line) in THF at 298 K.

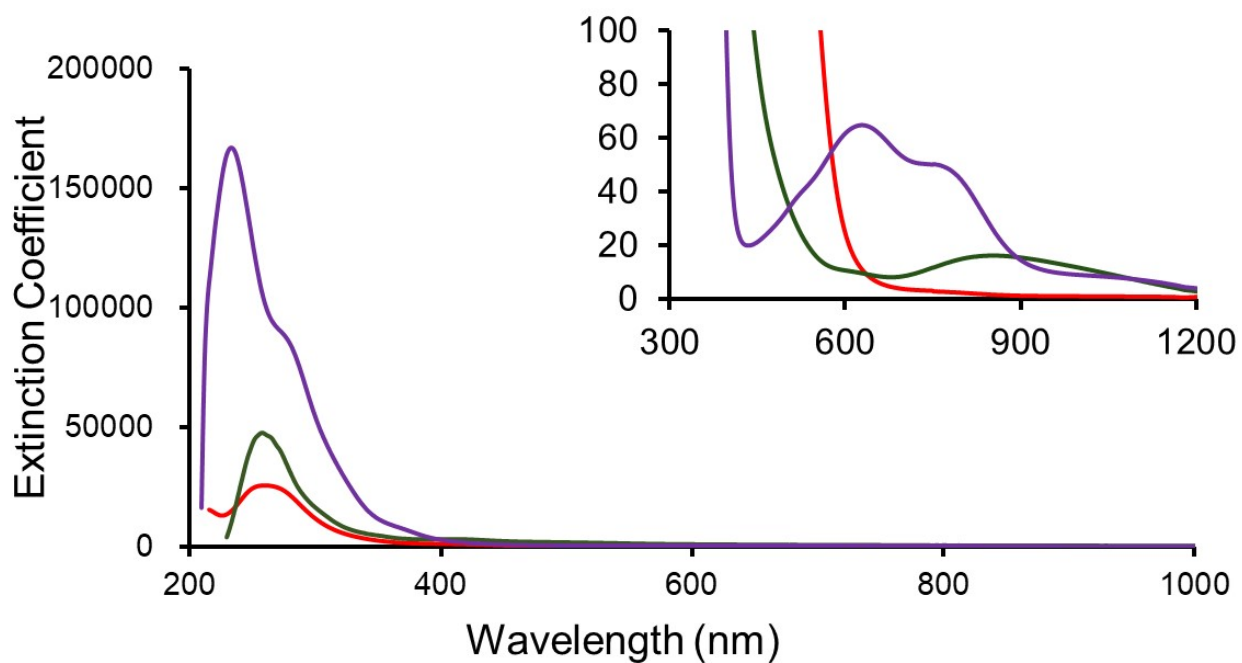


Figure S12. UV-Vis spectra of $\text{Cp}^*_2\text{Ti}(\text{C}_2\text{H}_4\text{CO}_2)$ (**2**, red line), $[\text{Na}(\text{THF})_2][\text{Cp}^*_2\text{Ti}(\text{C}_2\text{H}_4\text{CO}_2)]$ (**6**, green line), $\text{Cp}^*_2\text{Ti}(\text{O}_2\text{CCH}=\text{CH}_2)$ (**7**, purple line) in THF at 298 K.

V. IR Spectra

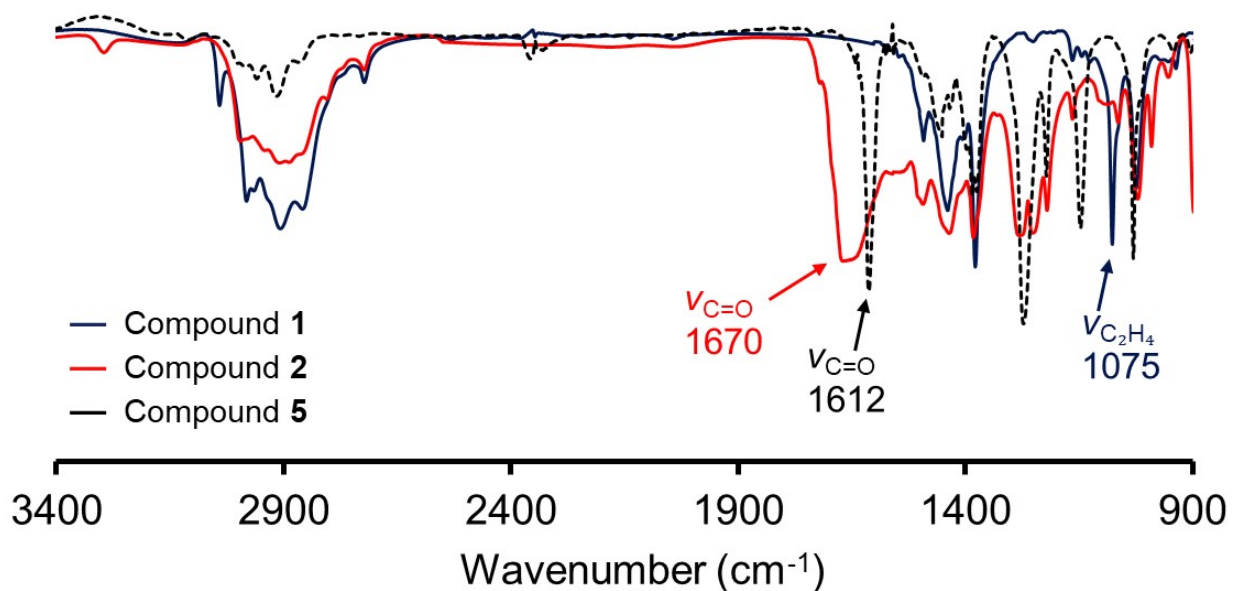


Figure S13. IR spectra of $\text{Cp}^*_2\text{Ti}(\text{C}_2\text{H}_4)$ (**1**, blue line), $\text{Cp}^*_2\text{Ti}(\text{C}_2\text{H}_4\text{CO}_2)$ (**2**, red line) and $[\text{Cp}^*_2\text{Ti}(\text{C}_2\text{H}_4\text{CO}_2\text{Me})][\text{OTf}]$ (**5**, black line) (KBr pellet).

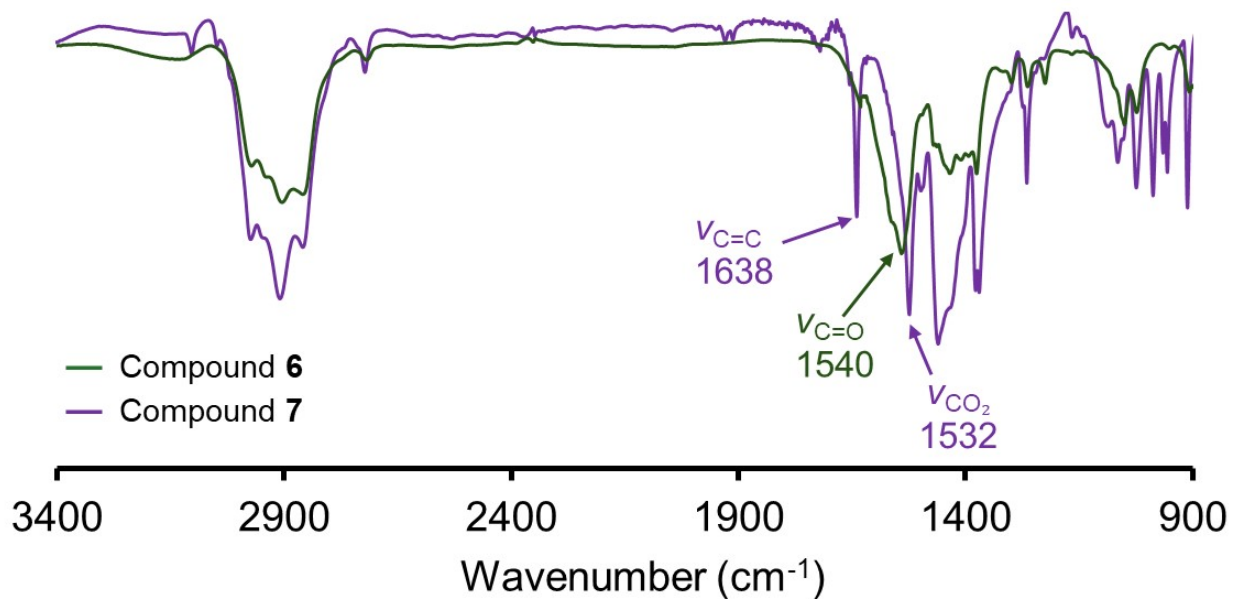


Figure S14. IR spectra of $[\text{Na}(\text{THF})_2][\text{Cp}^*_2\text{Ti}(\text{C}_2\text{H}_4\text{CO}_2)]$ (**6**, green line) and $\text{Cp}^*_2\text{Ti}(\text{O}_2\text{CCH}=\text{CH}_2)$ (**7**, purple line) (KBr pellet).

VI. Kinetic Studies on Formation of **2**

The reaction was performed in a 1 cm UV cuvette by monitoring UV-Vis spectral changes of reaction solutions under N₂ atmosphere. Rate constants were determined by fitting the absorbance changes at 410 nm for the formation of **2**. After completion of the reaction, the kinetic data were fitted to a pseudo-first-order model, allowing for the determination of the k_{obs} values.

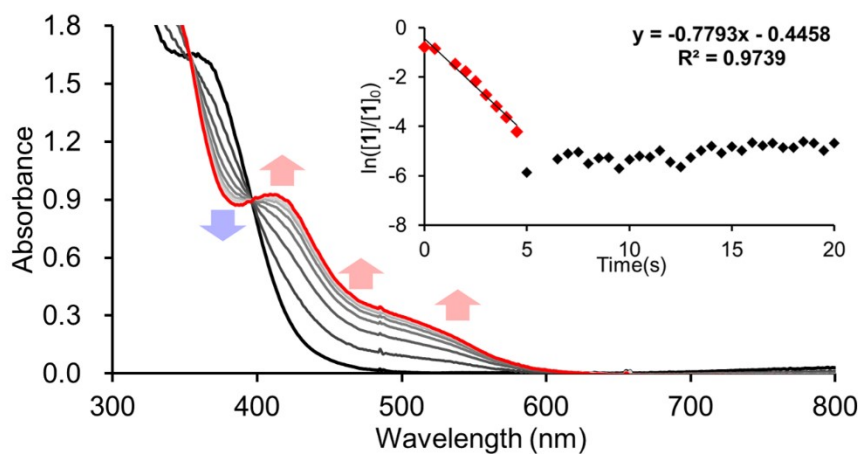


Figure S15. UV-Vis spectral changes of **1** (black line) to **2** (red line) upon addition of CO₂ to **1** at 273 K.

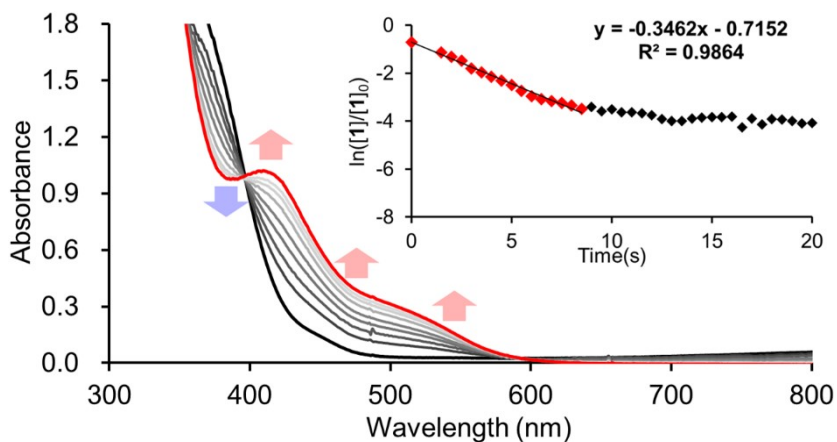


Figure S16. UV-Vis spectral changes of **1** (black line) to **2** (red line) upon addition of CO₂ to **1** at 253 K.

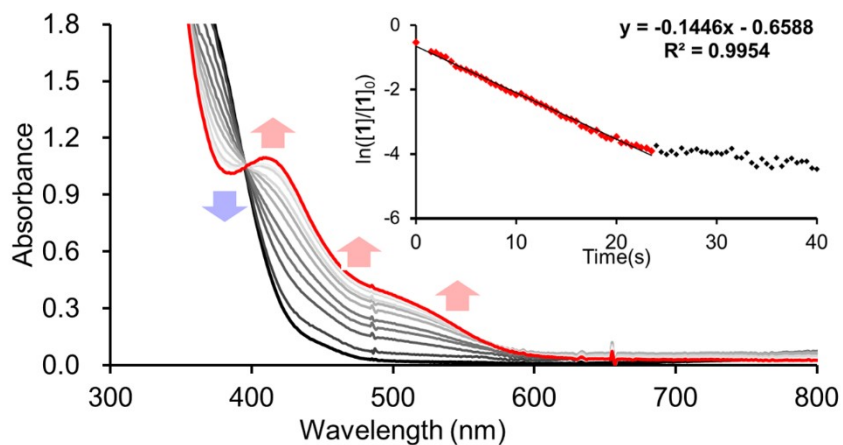


Figure S17. UV-Vis spectral changes of **1** (black line) to **2** (red line) upon addition of CO₂ to **1** at 233 K

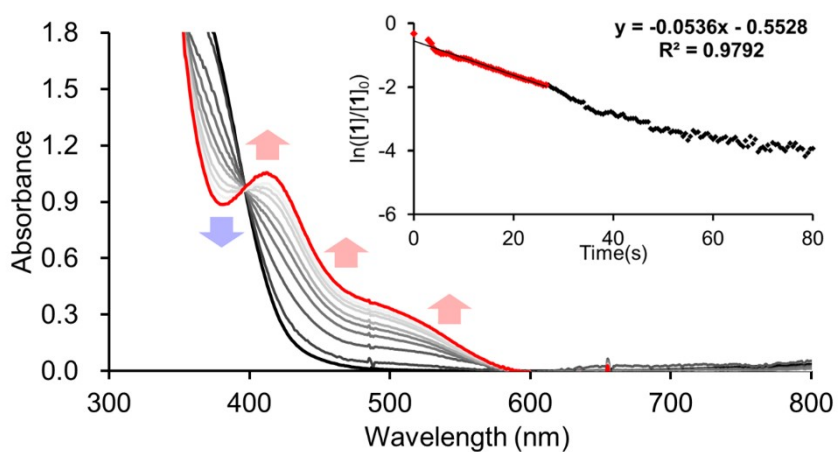


Figure S18. UV-Vis spectral changes of **1** (black line) to **2** (red line) upon addition of CO₂ to **1** at 213 K

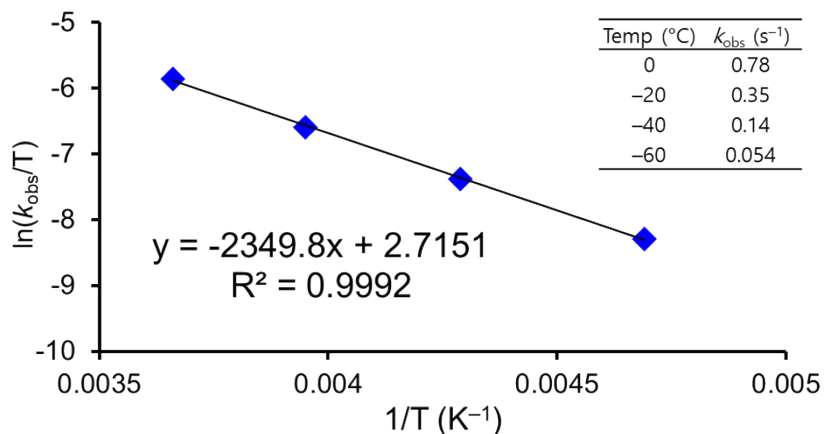
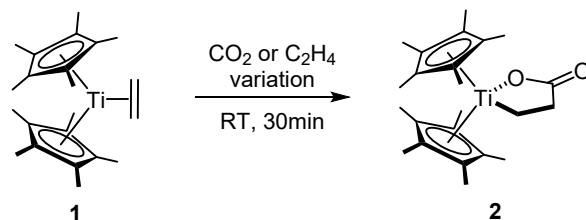


Figure S19. Eyring plot constructed using k_{obs} values measured at 0, -20, -40 and -60 °C.

VII. Formation of 2 with Varying C₂H₄ and CO₂ Equivalents



A stock solution of Cp*₂Ti(C₂H₄) (**1**, 132 mg, 0.381 mmol) and Ph₃Me (93 mg, 0.38 mmol) was prepared in 44 mL of toluene. A 10 mL aliquot of the stock solution was transferred to 100 mL Schlenk flask. A desired amount of C₂H₄(g) was injected directly into the solution using a syringe. After 30 min, a desired amount of CO₂(g) was injected directly into the solution using a syringe. The reaction mixture was stirred at room temperature for 30 min. The volatile was removed under vacuum and the resulting residue was dissolved in C₆D₆ and analyzed by ¹H NMR spectroscopy. The yield of compound **2** was determined by comparing the relative integration of the methylene signal of Cp*₂Ti(C₂H₄CO₂) and the internal standard (Ph₃Me).

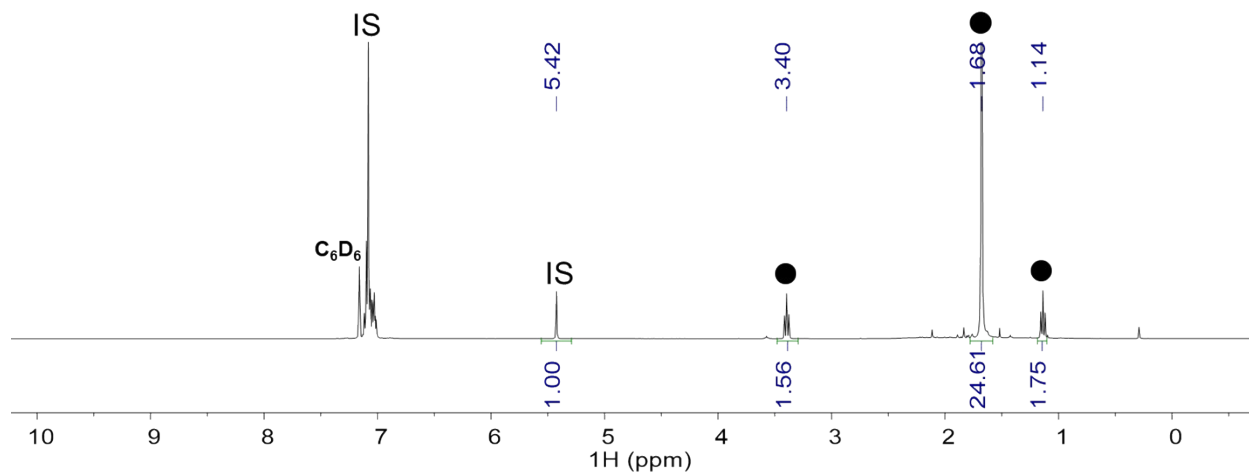


Figure S20. ¹H NMR spectrum of reaction mixture of **1** with varying C₂H₄/CO₂ equivalent (Table S1 Entry 9) in C₆D₆. (●: Compound **2**, IS: Ph₃Me internal standard)

Table S1. Effect of C₂H₄ and CO₂ on the formation of **2**.

Entry	C ₂ H ₄ (equiv)	CO ₂ (equiv)	Yield of 2 (%) ^a	Entry	C ₂ H ₄ (equiv)	CO ₂ (equiv)	Yield of 2 (%) ^a
1	-	1	58(6)	9	5	20	98
2	-	5	76(3)	10	10	10	78(1)
3	-	10	79(5)	11	20	20	76(1)
4	-	20	80(6)	12	50	1	71
5	1	1	60(4)	13	50	5	57
6	5	1	72	14	50	10	56
7	5	5	79(7)	15	50	20	40
8	5	10	84				

[a] Standard deviation in parenthesis

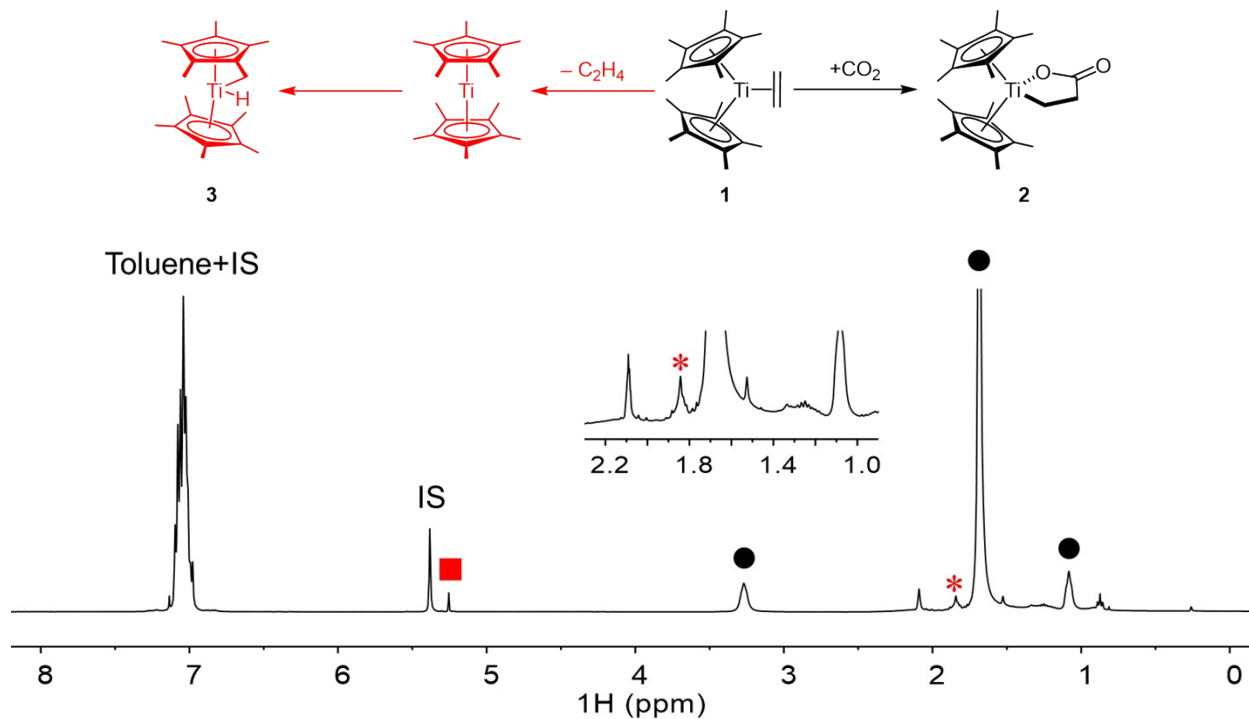


Figure S21. ¹H NMR spectrum of reaction mixture of **1** with CO₂ in toluene-*d*₈ (●: Compound **2**, ■: free C₂H₄, *: Compound **3**, IS: Ph₃Me internal standard).

VIII. Conversion of **5** to Methyl Acrylate and PMA

A solution of **5** (10 mM) and triphenylmethane (10 mM) in CDCl₃ was prepared and transferred into a J-Young NMR tube. Time-resolved ¹H NMR spectra (600 MHz) were recorded at selected time points, while keeping all instrumental parameters constant.

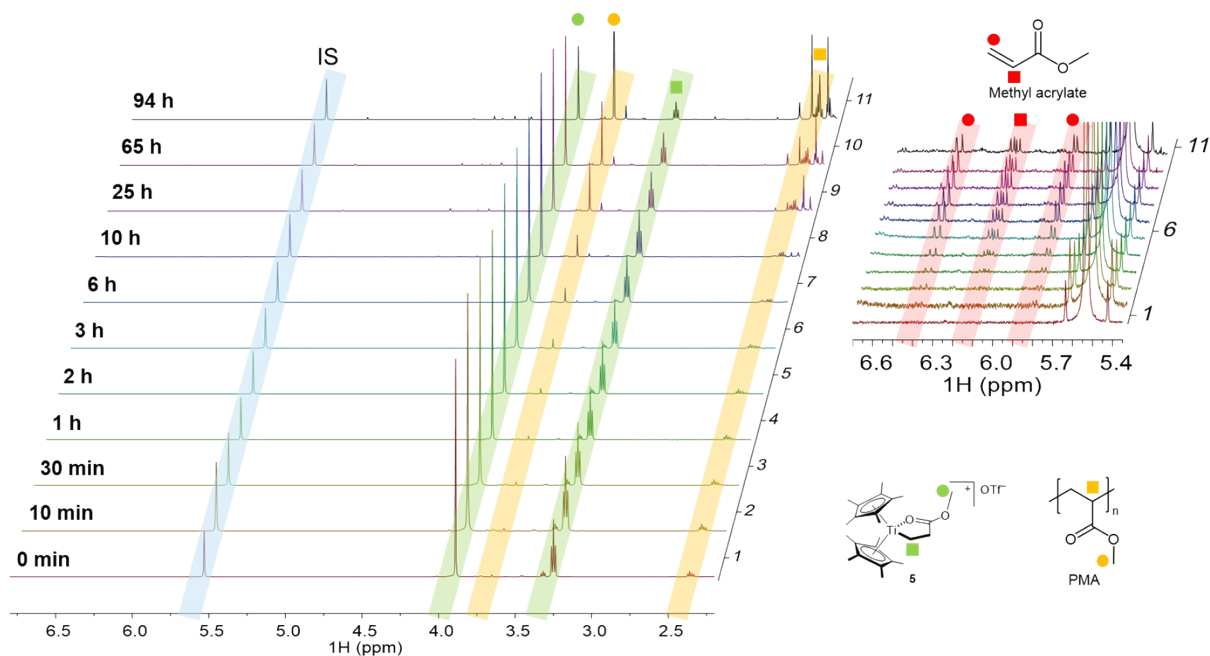


Figure S22. Time-resolved ¹H NMR spectra acquired during heating of **5** in CDCl₃ at 60 °C. Compound **5**, methyl acrylate, poly(methyl acrylate) and internal standard signals are highlighted with a green, red, yellow and blue, respectively.

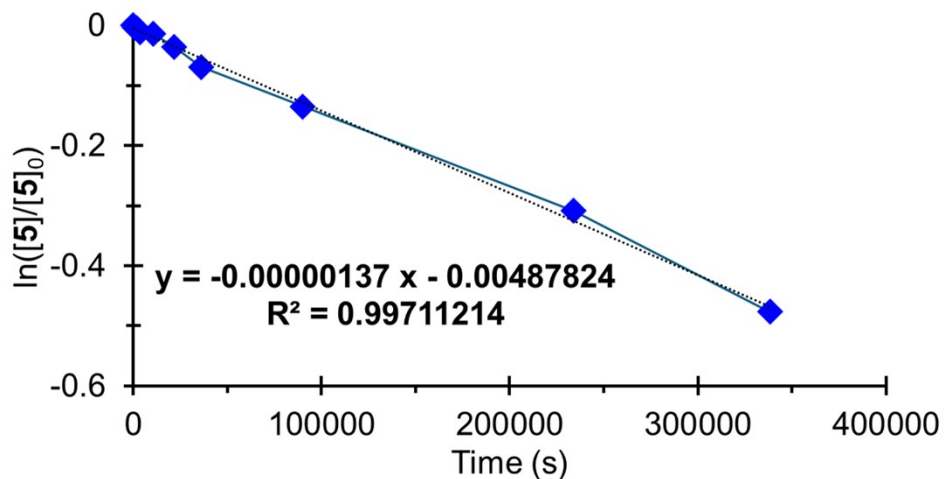


Figure S23. First-order kinetic plot for conversion of **5** in CDCl₃ at 60 °C.

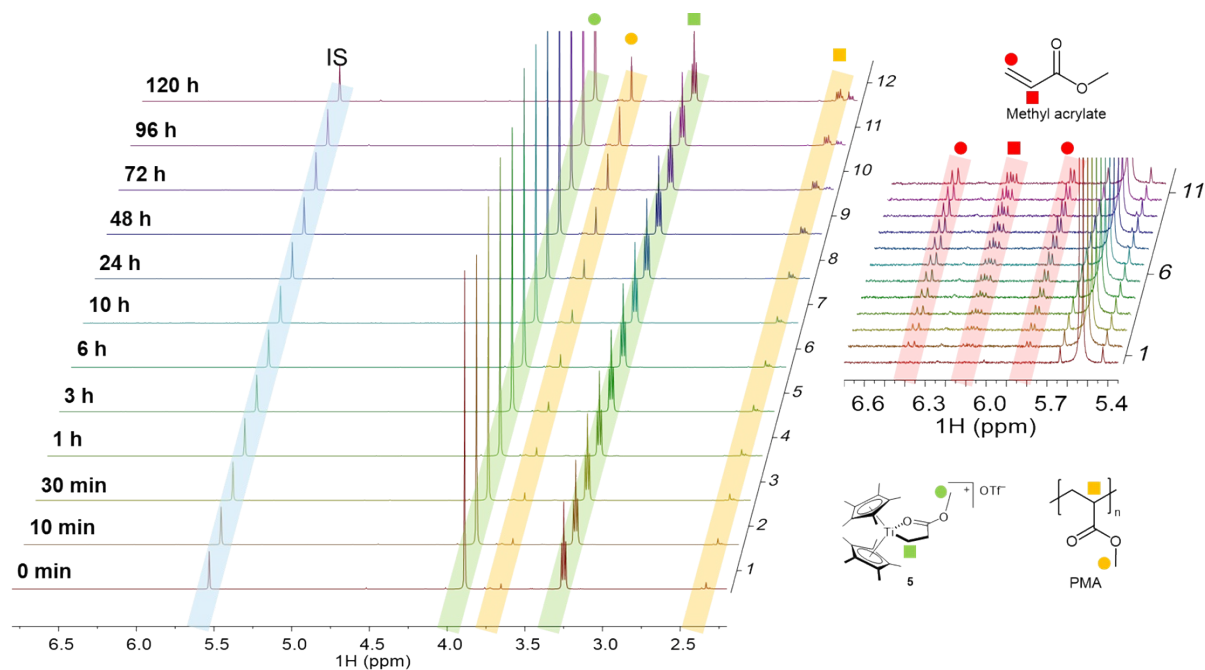


Figure S24. Time-resolved ^1H NMR spectra acquired during heating of **5** in CDCl_3 at $50\text{ }^\circ\text{C}$. **5**, methyl acrylate, poly(methyl acrylate) and internal standard signals are highlighted with a green, red, yellow and blue, respectively.

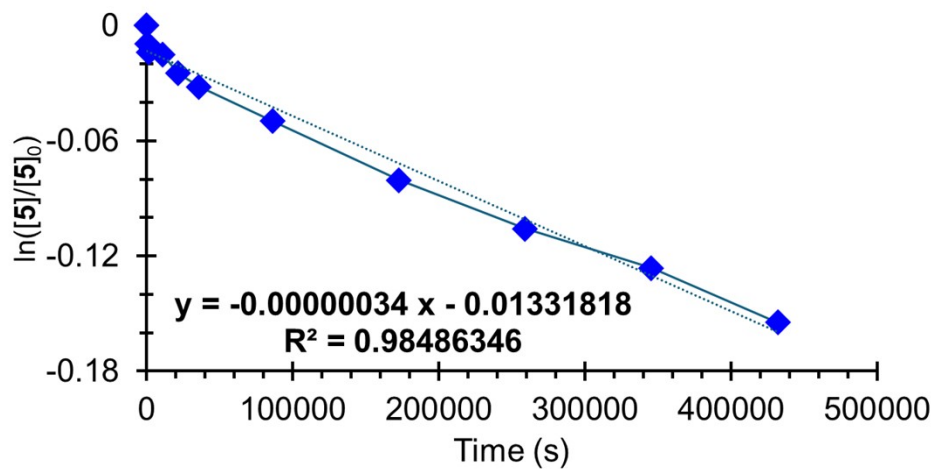


Figure S25. First-order kinetic plot for conversion of **5** in CDCl_3 at $50\text{ }^\circ\text{C}$.

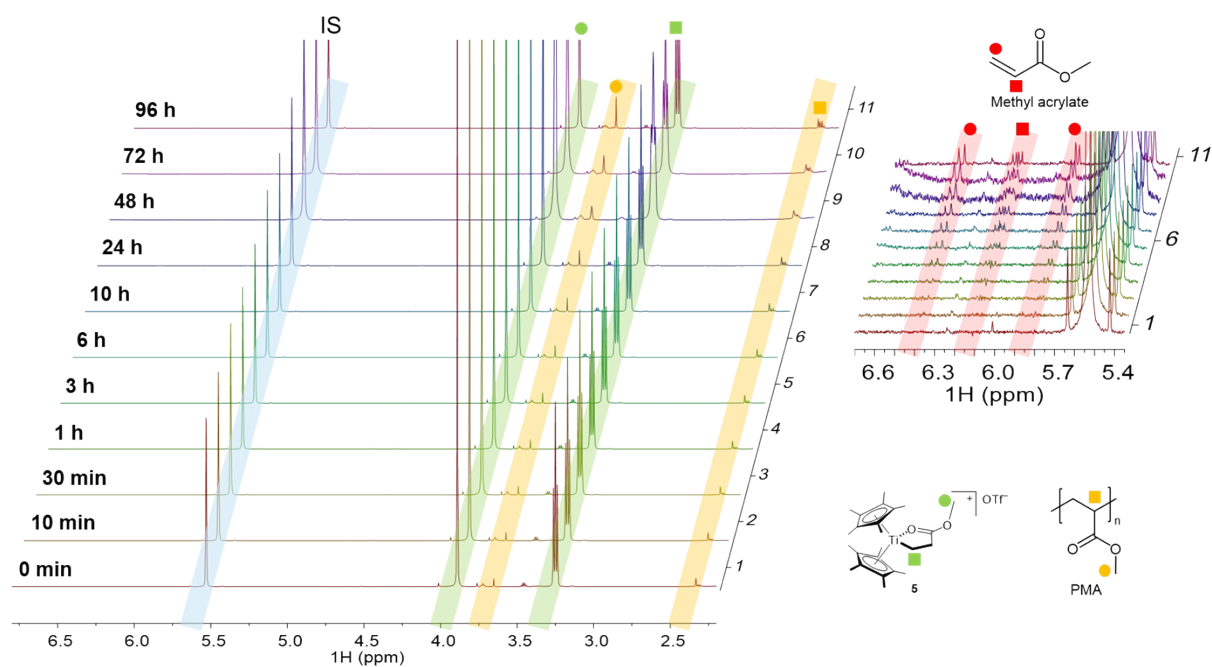


Figure S26. Time-resolved ^1H NMR spectra acquired during heating of **5** in CDCl_3 at $40\text{ }^\circ\text{C}$. **5**, methyl acrylate, poly(methyl acrylate) and internal standard signals are highlighted with a green, red, yellow and blue, respectively.

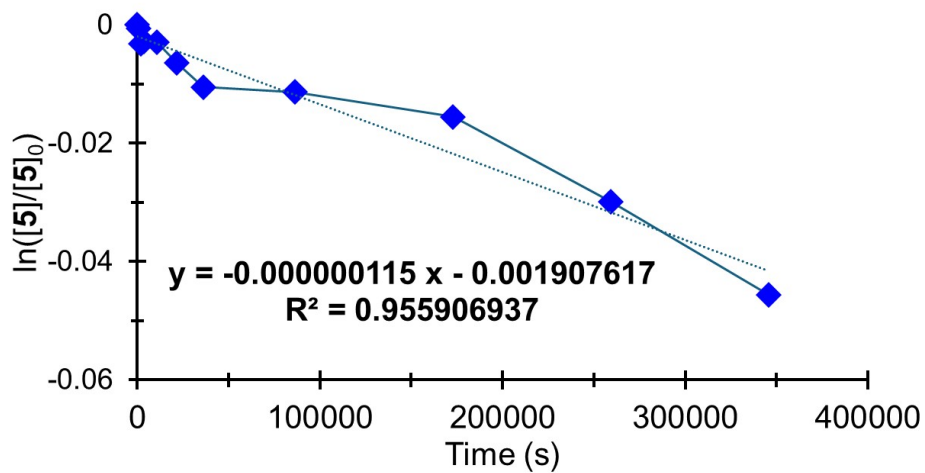


Figure S27. First-order kinetic plot for conversion of **5** in CDCl_3 at $40\text{ }^\circ\text{C}$.

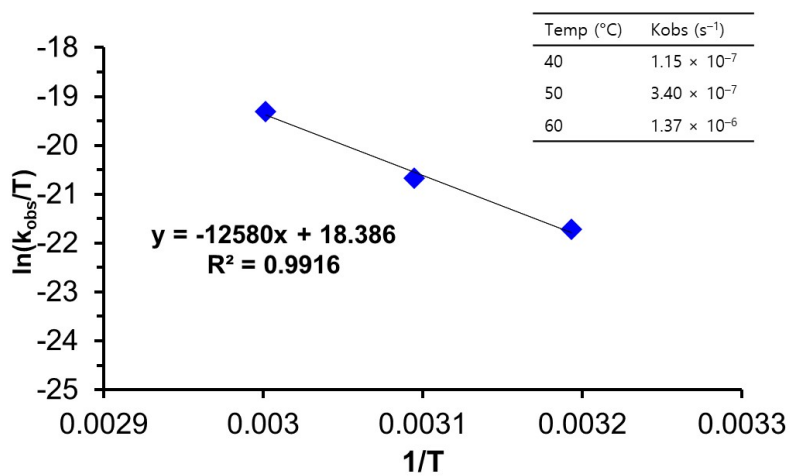
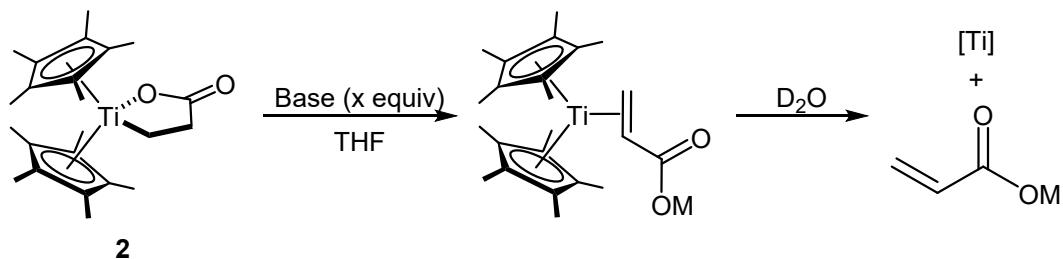


Figure S28. Eyring plot constructed using k_{obs} values for consumption of **5** measured at 40, 50, and 60 °C.

IX. Deprotonation of **2**



To a solution of $\text{Cp}^*_2\text{Ti}(\text{C}_2\text{H}_4\text{CO}_2)$ (**2**, 30 mg, 0.077 mmol) in 2 mL solvent were added base. The reaction mixture was stirred for the desired time at room temperature. The reaction mixture was brought out of the glovebox and was diluted with 10 mL diethyl ether. The acrylate was extracted with 2 mL D_2O . 20 μM 3-(trimethylsilyl)propionic-2,2,3,3- d_4 acid sodium salt solution (430 μL , 0.009 mmol) was added as an internal standard for ^1H NMR analysis. The amount of acrylate produced is determined by relative integration of acrylate signals and the area of the trimethyl signal of the internal standard.

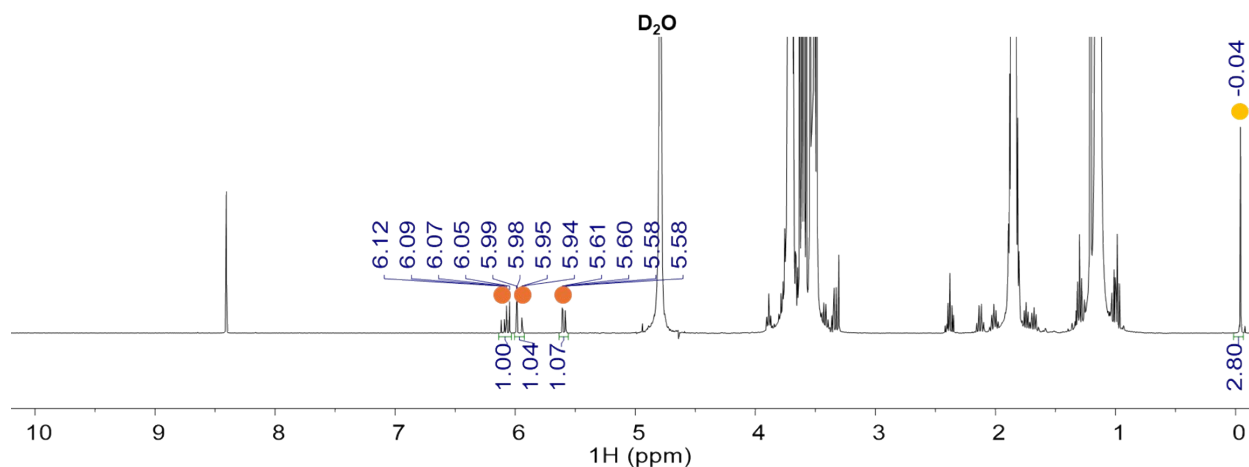


Figure S29. ^1H NMR spectrum of reaction **2** with base (Table S2, Entry 15) in D_2O (●: acrylate, ●: internal standard (3-(trimethylsilyl)propionic-2,2,3,3- d_4 acid sodium salt)).

Table S2. Effect of base on deprotonation of **2**.

Entry	Base	pK_a^{7-11} (in MeCN)	Solvent	Additive	Acrylate Yield (%) ^a
1	NaOH	15.7	THF	-	-
2	NEt ₃	18.83	THF	NaBAr ^F ₄	-
3	DBU	24.31	THF	NaBAr ^F ₄	-
4	Na-2-fluorophenolate	25.36	THF	-	-
5	^t BuP1(pyrr) ₃	28.42	THF	NaBAr ^F ₄	0.01
6	Isopropyl Verkade base	33.63	THF	NaBAr ^F ₄	-
7	LiHMDS	~34	THF		0.04
8	NaHMDS	~34	THF	-	0.01
9	KHMDS	~34	THF		0.01
10	NaOMe	~37	THF	-	11
11	NaO ^t Pr	~39	THF	-	11
12	LiO ^t Bu	~40	THF	-	15(0.3)
13	KO ^t Bu	~40	THF	-	24(11)
14	NaO ^t Bu	~40	THF	-	24
15	NaO ^t Bu (10 equiv)		THF	-	39(1)
16	NaO ^t Bu (20 equiv)		THF	-	40
17	NaO ^t Bu		Tol	-	10
18	NaO ^t Bu		MeCN	-	9
19	NaO ^t Bu		CHP	-	-
20	NaO ^t Bu		THF	PCy ₃	10
21	NaO ^t Bu		THF	C ₂ H ₄	12
22	NaO ^t Bu (10 equiv)		THF	AgOTf	25
23	NaO ^t Bu (10 equiv)		THF	[C ₇ H ₇][BF ₄]	15
24	NaO ^t Bu (10 equiv)		THF	[Cp ₂ Co][PF ₆]	72(0.7)

[a] Standard deviation in parenthesis.

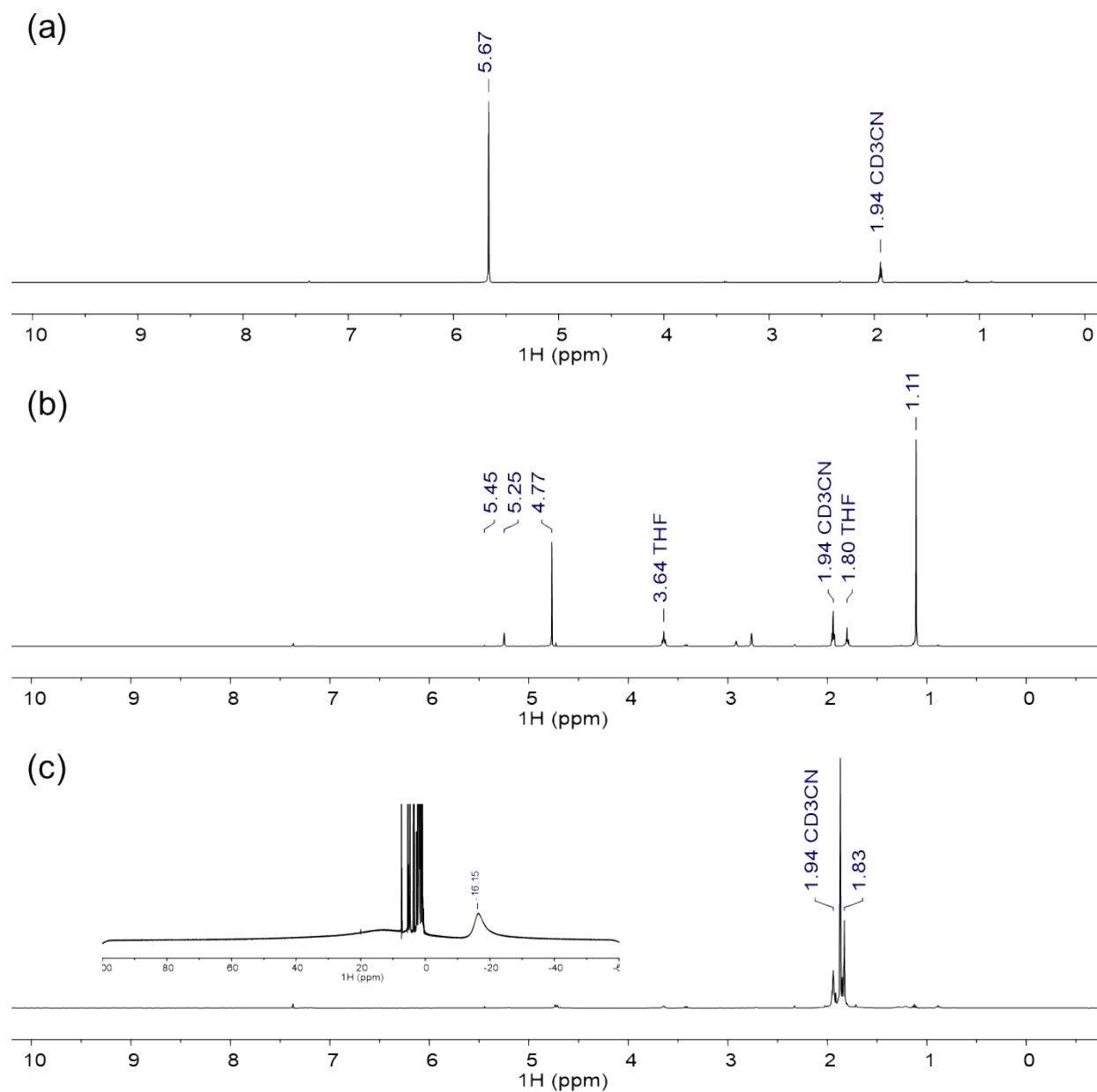


Figure S30. Control experiments for $[\text{Cp}_2\text{Co}][\text{PF}_6]$ reactivity. ^1H NMR spectra (CD_3CN , 298 K) of (a) $[\text{Cp}_2\text{Co}][\text{PF}_6]$ alone; (b) $[\text{Cp}_2\text{Co}][\text{PF}_6] + \text{NaO}^t\text{Bu}$; (c) $[\text{Cp}_2\text{Co}][\text{PF}_6] + \text{Compound 1}$. Inset in (c): wide-range spectrum showing a paramagnetic resonance at $\delta -16.15$.

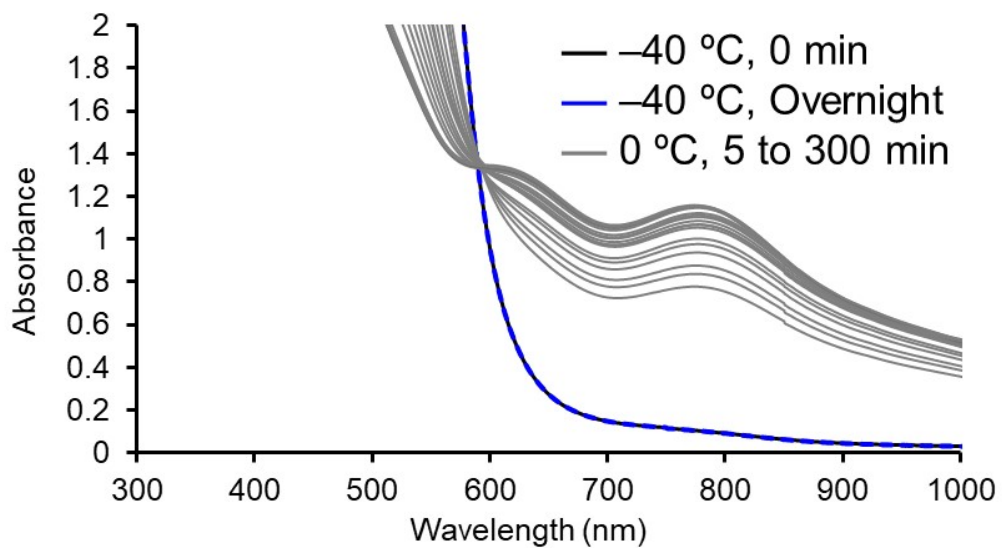
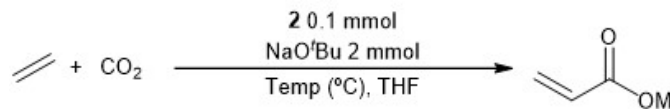


Figure S31. A low temperature UV-Vis spectra of deprotonation of **2** with NaO^tBu (10 equiv). No spectral change was observed at $-40\text{ }^{\circ}\text{C}$ overnight. At $0\text{ }^{\circ}\text{C}$, the reaction proceeded, but only the Ti(III) species **6** and **7** were observed to accumulate without any observation of other intermediate.

X. Catalytic Acrylate Synthesis



The catalytic experiments were conducted using the Parr Series 5000 Multiple Reactor System. In an N₂-filled glovebox, compound **2** (39.0 mg, 0.1 mmol) was added to a 20 mL oven-dried scintillation vial, along with 2 mmol of NaO^tBu and 10 mL of THF. The vial was inserted into the reactor, which was assembled and removed from the glovebox. The reactor was purged 10 bar of C₂H₄ three times and then filled with predetermined amounts of C₂H₄ and CO₂. The ethylene carboxylation was carried out under the desired temperature. After reaction, the reactor was cooled to room temperature, and the pressure was released. The reactor was disassembled, 3-(Trimethylsilyl)propionic-2,2,3,3-*d*₄ acid sodium salt (13.7 mg, 0.08 mmol) in 10 mL of D₂O was added as an internal standard. 10 mL of diethyl ether was added to the reaction mixture, then an aliquot of D₂O phase was analyzed using ¹H NMR.

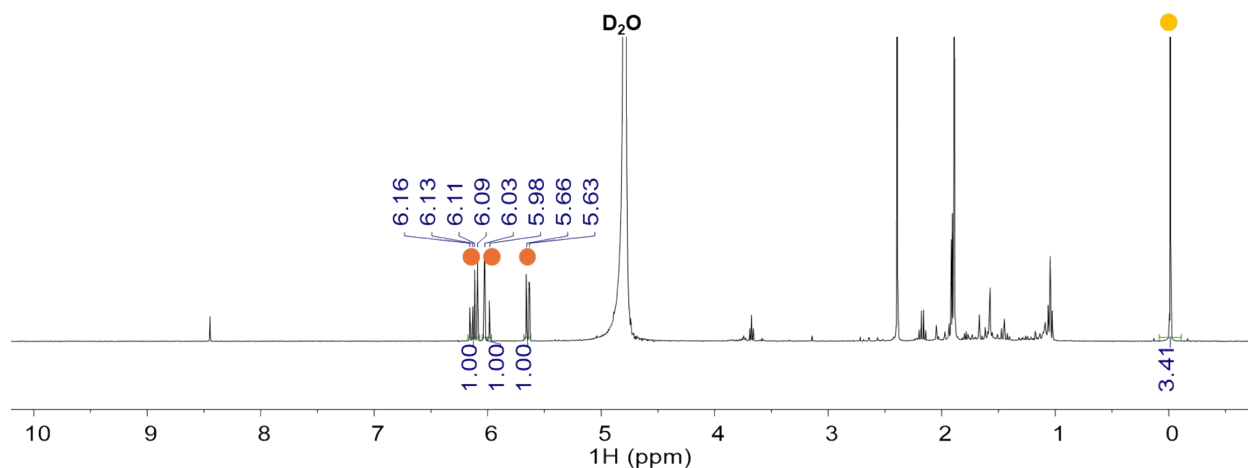


Figure S32. ¹H NMR spectrum in D₂O of the crude mixture of synthesis of acrylate at catalytic condition (Table 3, entry 2) (● : acrylate, ● : Internal standard (3-(trimethylsilyl)propionic-2,2,3,3-*d*₄ acid sodium salt))

XI. Crystallographic Details

The diffraction data of **2**, **5** and **6** were collected on a Bruker D8 QUEST. The data were collected with Mo K α radiation ($\lambda = 0.71073 \text{ \AA}$) at 100 K. Bruker APEX4 software program was used for data collection, cell refinement, reduction and absorption correction. The diffraction data of **7** were collected on Rayonix MX225HS CCD area detector at 2D SMC at the Pohang Accelerator Laboratory, Korea. The data were collected with Si(111) double crystal monochromated synchrotron radiation ($\lambda = 0.70000 \text{ \AA}$) at 100 K. The PAL BL2D-SMDC Program¹² was used for data collection and HKL3000sm¹³ was used for cell refinement, reduction and absorption correction. The structures were solved by direct methods and all nonhydrogen atoms were subjected to anisotropic refinement by full-matrix least-squares on F^2 using the SHELXTL/PC package.¹⁴ Hydrogen atoms were placed at their geometrically calculated positions and refined riding on the corresponding carbon atoms with isotropic thermal parameters. Full crystallographic details can be obtained free of charge from the Cambridge Crystallographic Data Center via www.ccdc.cam.ac.uk/data_request/cif (CCDC 2463344-2463347).

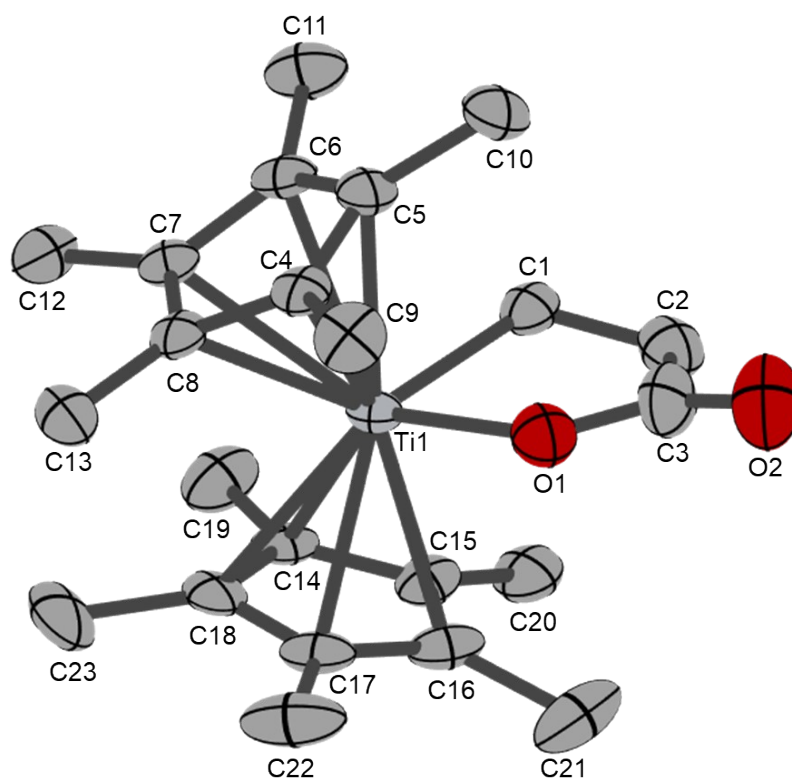


Figure S33. Structural representation of **2** with ellipsoids drawn at 50% probability level. Hydrogen atoms on the ligand are omitted for clarity.

Bond distance (Å)		Bond Angle (°)	
Ti1–C1	2.149(5)	Ti1–O1–C3	120.8(3)
Ti1–O1	2.015(3)	O1–C3–O2	119.4(5)
C2–C3	1.519(8)		
C3–O1	1.317(7)		
C3–O2	1.231(6)		

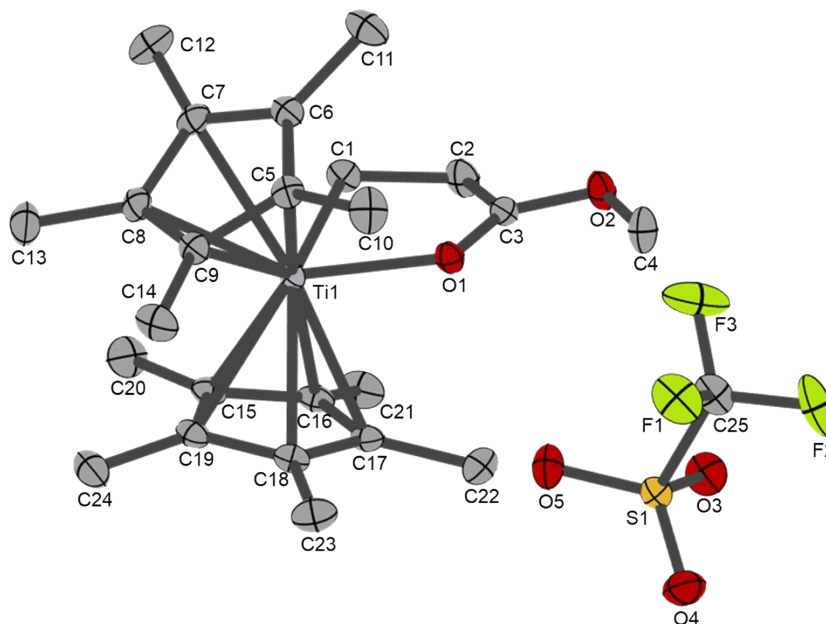


Figure S34. Structural representation of **5** with ellipsoids drawn at 50% probability level. The asymmetric unit cell contains two pairs of **5**. For clarity, one pair of **5** is presented. Hydrogen atoms on the ligand are omitted for clarity.

Bond distance (Å)		Bond Angle (°)	
Ti1–C1	2.224(2)	Ti1–O1–C3	117.80(3)
Ti1–O1	2.0845(14)	O1–C3–O2	121.11(18)
C2–C3	1.482(3)		
C3–O1	1.245(2)		
C3–O2	1.311(2)		
C4–O2	1.460(3)		

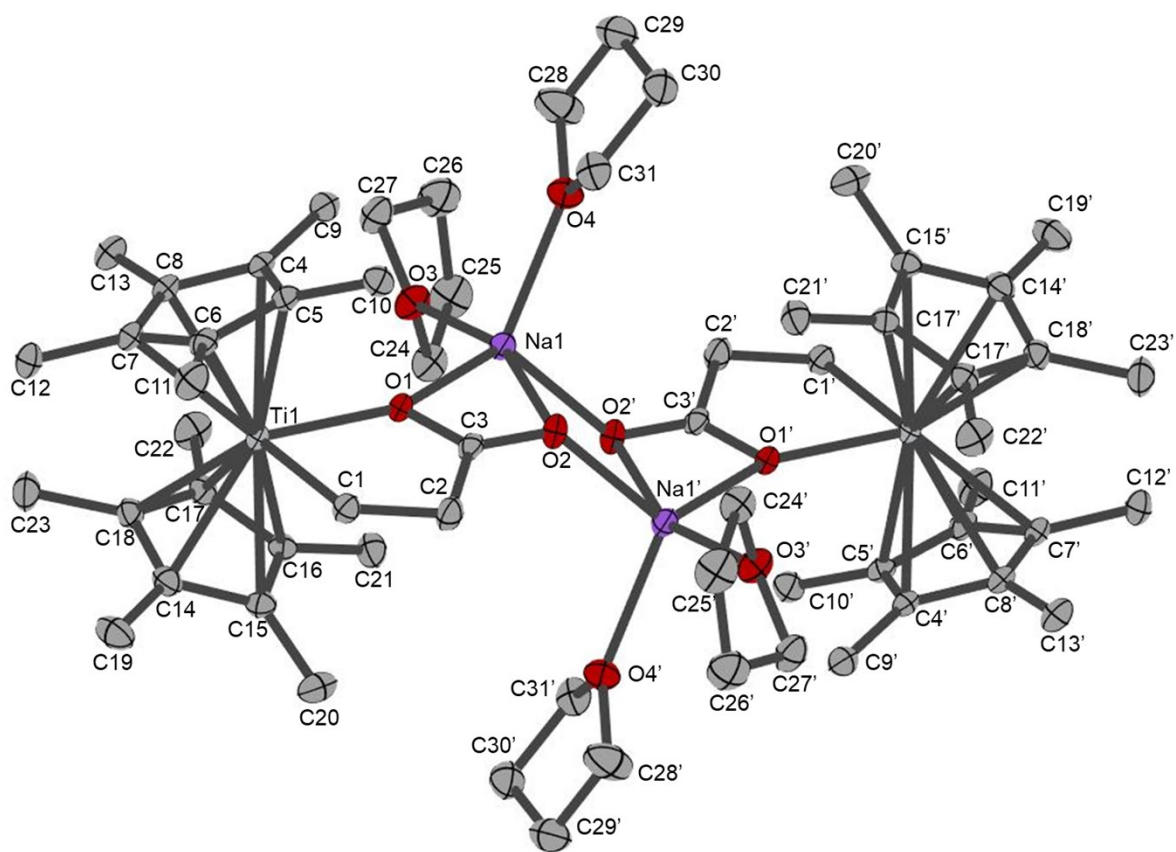


Figure S35. Structural representation of **6** with ellipsoids drawn at 50% probability level. Hydrogen atoms on the ligand are omitted for clarity.

Bond distance (Å)		Bond Angle (°)	
Ti1–C1	2.2542(15)	Ti1–O1–C3	120.83(9)
Ti1–O1	2.1463(10)	O1–C3–O2	121.22(13)
C2–C3	1.514(2)		
C3–O1	1.2770(17)		
C3–O2	1.2612(17)		

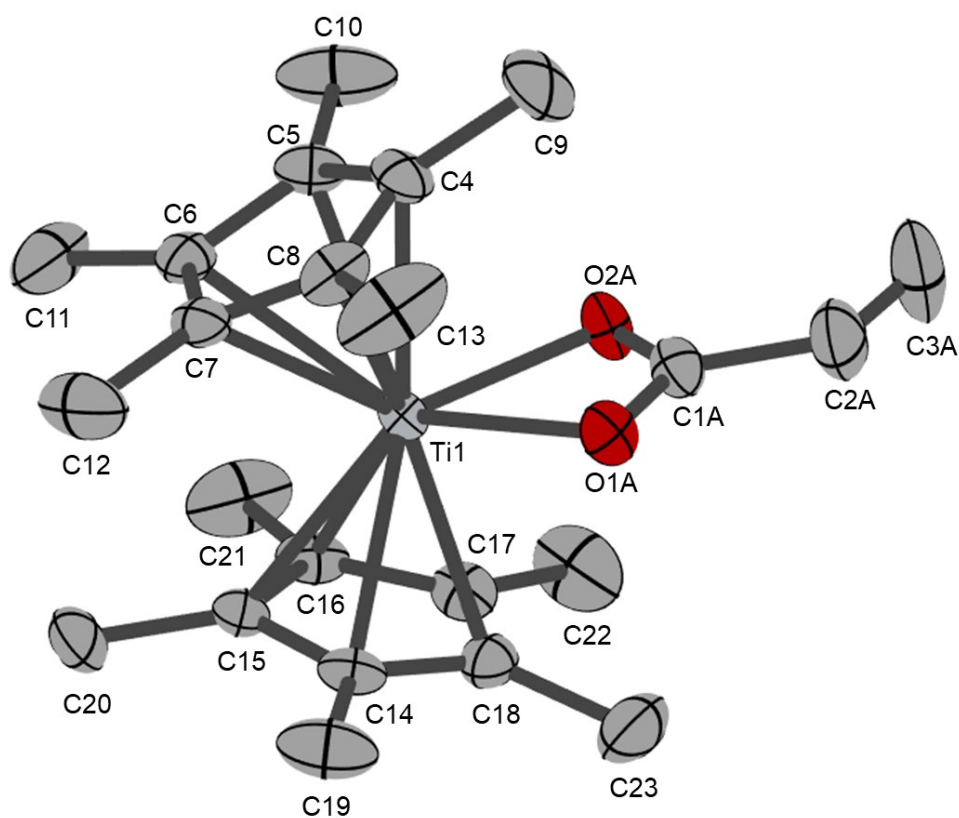


Figure S36. Structural representation of **7** with ellipsoids drawn at 50% probability level. The acrylate group was disordered over two distinct positions with occupancies of 0.871(7) and 0.129(7). For clarity, only one component is shown. Hydrogen atoms on the ligand are omitted for clarity.

Bond distance (Å)			Bond Angle (°)		
	Major (0.871)	Minor (0.129)		Major (0.871)	Minor (0.129)
Ti1–O1	2.188(3)	2.208(18)	O1–C1–O2	119.5(4)	120(3)
Ti1–O2	2.173(3)	2.101(19)	O1–Ti1–O2	60.32(10)	60.8(7)
O1–C1	1.270(5)	1.21(4)	C1–C2–C3	123.1(4),	123(3)
O2–C1	1.266(5)	1.30(4)			
C2–C3	1.311(7)	1.30(5)			

XII. Cyclic Voltammograms

Electrochemistry. Electrochemical measurements were carried out in a glovebox under a N₂ atmosphere using an AMETEK VersaSTAT3 Potentiostat/Galvanostat. A glassy carbon electrode was used as the working electrode and a platinum wire was used as the auxiliary electrode. The reference electrode was Ag/AgNO₃ in an electrolyte solution. The ferrocene couple FeCp₂/FeCp₂⁺ was used as an external reference.

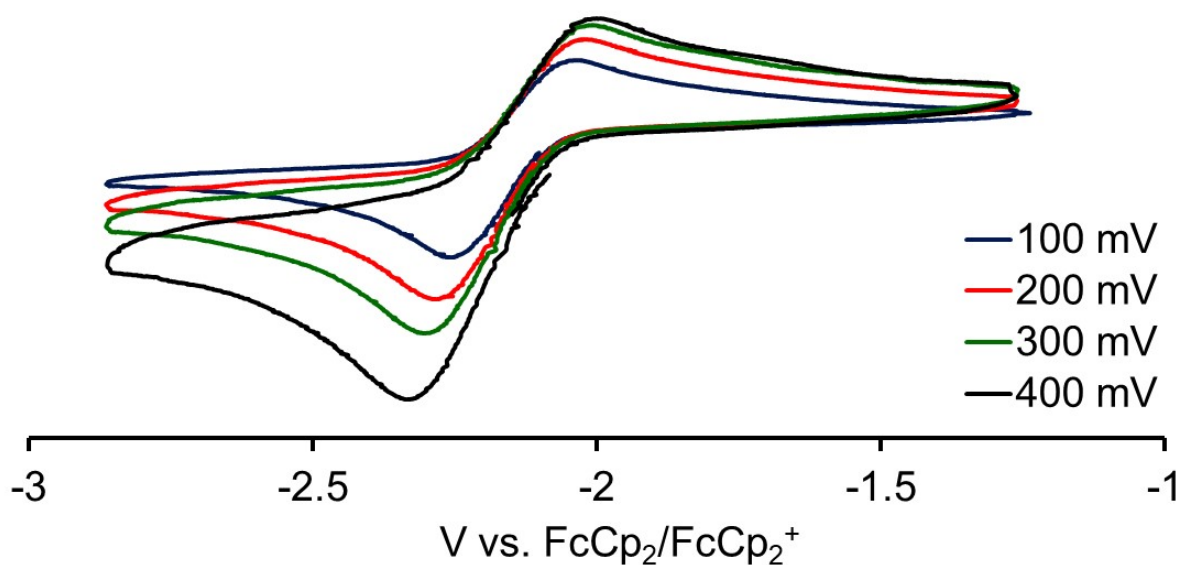


Figure S37. Cyclic voltammogram of Cp*₂Ti(C₂H₄CO₂) (2) with scan rate: 100, 200, 300 and 400 mV/s. Ti^{IV/III} couple at -2.15 V vs Fc/Fc⁺ was observed in THF with 0.3 M tetra-*n*-butylammonium hexafluorophosphate as an electrolyte.

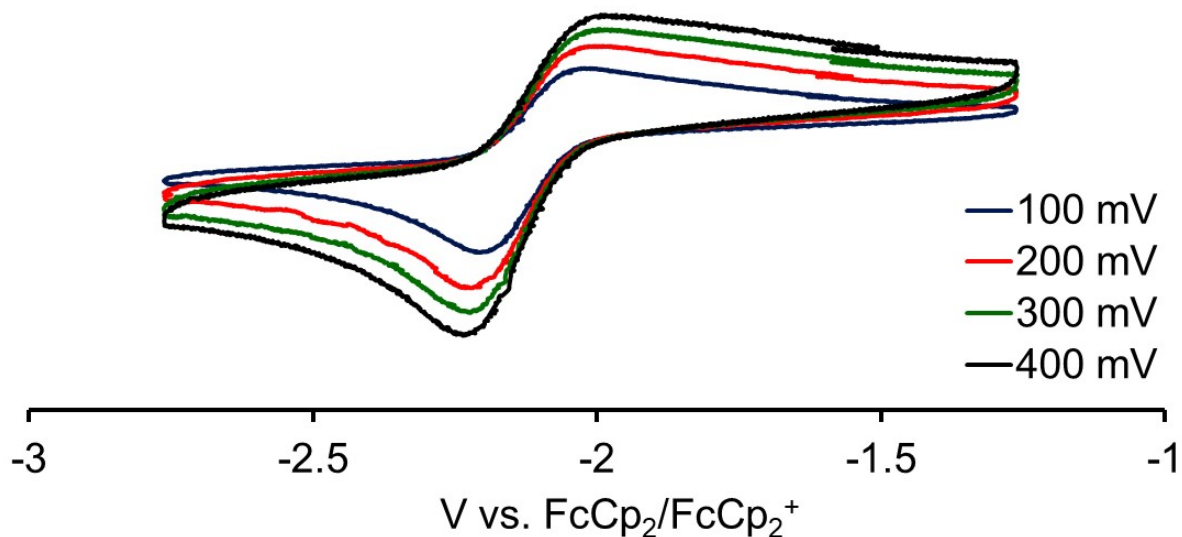


Figure S38. Cyclic voltammogram of $[\text{Na}(\text{THF})_2][\text{Cp}^*_2\text{Ti}(\text{C}_2\text{H}_4\text{CO}_2)]$ (**6**) with scan rate: 100, 200, 300 and 400 mV/s. $\text{Ti}^{\text{IV/III}}$ couple at -2.10 V vs Fc/Fc^+ was observed in THF with 0.3 M tetra-*n*-butylammonium hexafluorophosphate as an electrolyte.

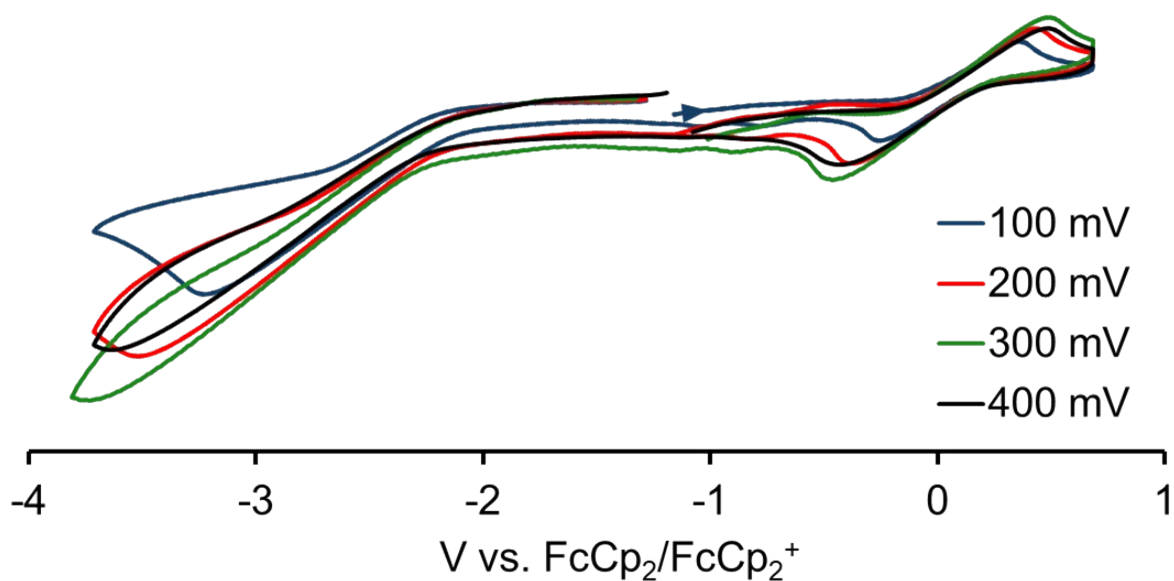


Figure S39. Cyclic voltammogram of $\text{Cp}^*_2\text{Ti}(\text{O}_2\text{CCH}=\text{CH}_2)$ (**7**) with scan rate: 100, 200, 300 and 400 mV/s. $\text{Ti}^{\text{IV/III}}$ couple at $+0.05$ V vs Fc/Fc^+ and $\text{Ti}^{\text{III/II}}$ reduction at -3.23 V vs Fc/Fc^+ were observed in THF with 0.3 M lithium perchlorate as an electrolyte.

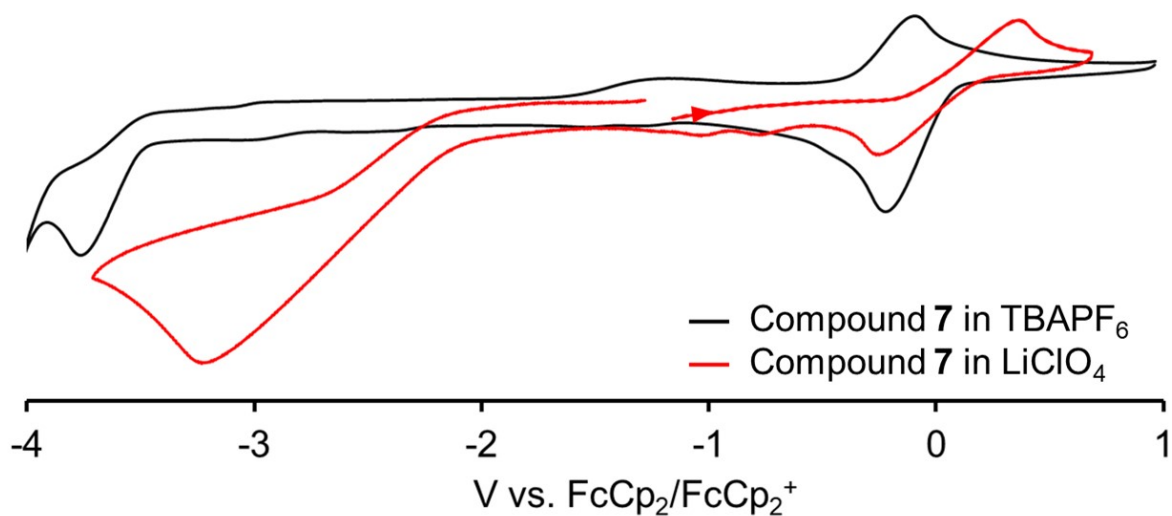


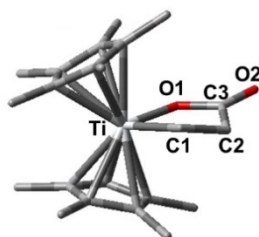
Figure S40. Cyclic voltammogram of $\text{Cp}^*_2\text{Ti}(\text{O}_2\text{CCH}=\text{CH}_2)$ (**7**) with scan rate 100 mV/s. $\text{Ti}^{\text{IV/III}}$ couple at +0.05 V vs Fc/Fc^+ and $\text{Ti}^{\text{III/II}}$ reduction at -3.23 V vs Fc/Fc^+ were observed in THF with 0.3 M lithium perchlorate as an electrolyte (Red), $\text{Ti}^{\text{IV/III}}$ couple at -0.16 V vs Fc/Fc^+ and $\text{Ti}^{\text{III/II}}$ reduction at -3.77 V vs Fc/Fc^+ were observed in THF with 0.3 M tetra-*n*-butylammonium hexafluorophosphate as an electrolyte. (Black)

XIII. DFT Calculation

Computational details.

All DFT computations were conducted with Gaussian 16-A03 software package,¹⁵ with the TPSS functional,¹⁶ the 6-311g(d,p) basis set,¹⁷⁻¹⁹ and the implicit CPCM solvation model²⁰ with $\epsilon = 7.426$ of tetrahydrofuran at 298 K and 1 atm. The transition states were confirmed by possessing only one imaginary frequency along the reaction coordinate, and further by intrinsic reaction coordinate (IRC) calculations.

Table S3. Selected bond lengths (in Å) of compound **2** obtained by X-ray crystallography and DFT optimization. Hydrogen atoms were omitted for clarity.



	Experimental (Å)	Computational (Å)
Ti-C1	2.149(5)	2.225
Ti-O1	2.016(4)	1.965
C1-C2	1.490(8)	1.537
C2-C3	1.519(7)	1.528
C3-O1	1.317(7)	1.334
C3-O2	1.230(7)	1.228

Table S4. DFT-computed M–O and M–C bond lengths of Pd(dmpe)(C₂H₄CO₂), Ni(NHC-P)(C₂H₄CO₂), and compound **2**. Wiberg bond indices were represented in parentheses. dmpe: 1,2-bis(dimethylphosphino)ethane, NHC-P: *N*-phosphino-methyl-*N*-heterocyclic carbene.

	Pd(dmpe)(C ₂ H ₄ CO ₂)	Ni(NHC-P)(C ₂ H ₄ CO ₂)	Compound 2
M–O	2.077 Å (0.435)	1.881 Å (0.276)	1.965 Å (0.557)
M–C	2.088 Å (0.629)	1.947 Å (0.553)	2.225 Å (0.701)

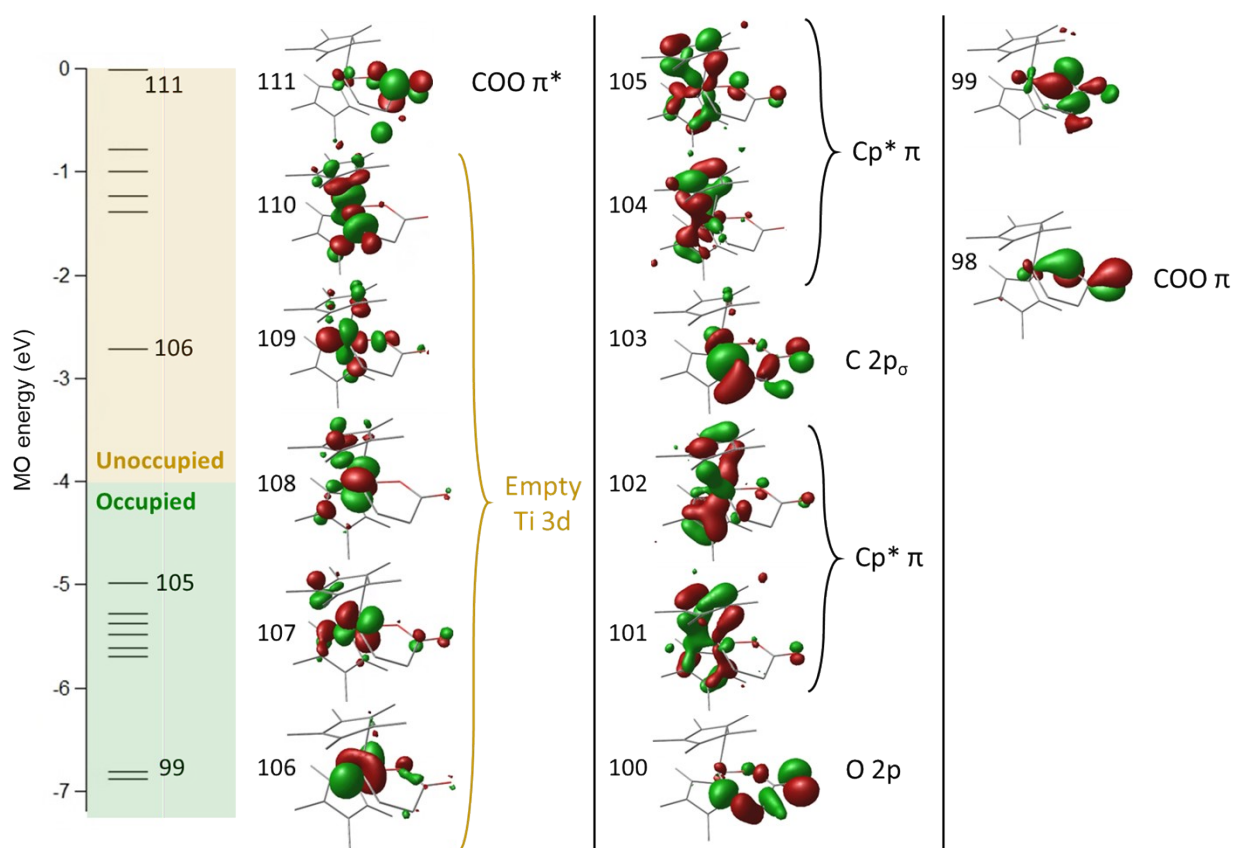
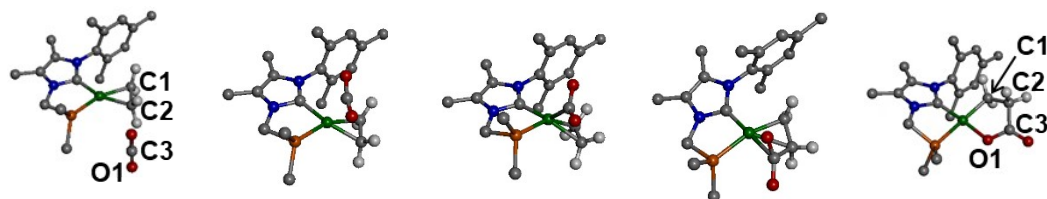


Figure S41. DFT-computed molecular orbitals and their energies of compound **2**.

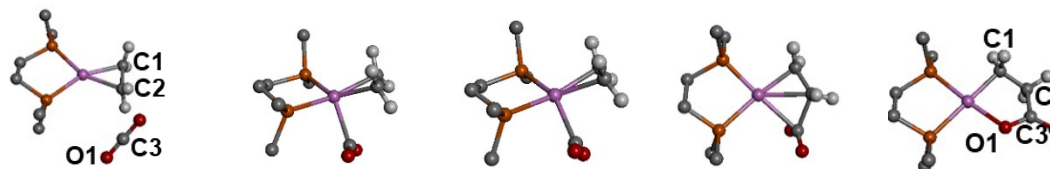
Reaction coordinate calculations

Table S5. DFT-computed reactant (R), intermediate (I), and product (P) of CO₂ carboxylation reaction of a Ni(NHC-P)(C₂H₄CO₂) complex. Protons other than from ethylene were omitted for clarity.



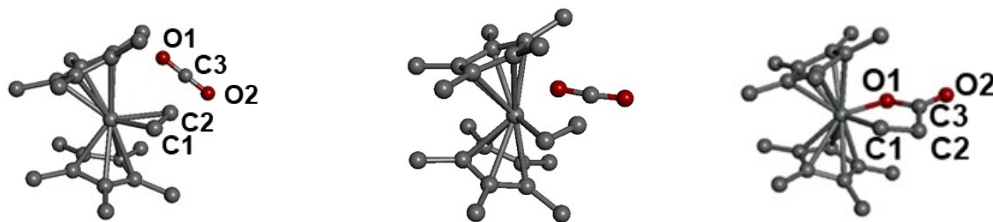
	CO ₂ coordination		CO ₂ insertion		
	R	TS	I	TS2	P
Ni–C3 (Å)	4.817	2.582	1.971	2.183	2.754
Ni–C1 (Å)	1.942	1.956	2.006	1.904	1.947
Ni–O1 (Å)	4.944	3.132	2.317	2.336	1.881
C1–C2 (Å)	1.440	1.434	1.411	1.496	1.535
C2–C3 (Å)	3.783	3.115	2.625	1.708	1.525
C3–O1 (Å)	1.170	1.187	1.224	1.268	1.324
ΔE (kcal/mol)	0.00	3.93	–0.09	13.29	–9.89
ΔH (kcal/mol)	0.00	3.10	–0.03	12.78	–8.81
ΔG (kcal/mol)	0.00	7.44	4.43	17.85	–3.68

Table S6. DFT-computed reactant (R), intermediate (I), and product (P) of CO₂ carboxylation reaction of a Pd(dmpe)(C₂H₄CO₂) complex. Protons other than from ethylene were omitted for clarity.



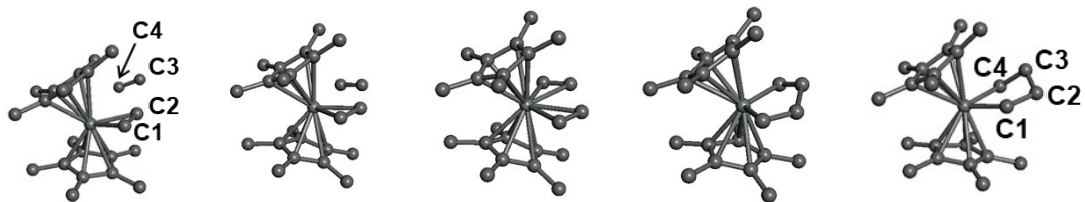
	CO ₂ coordination		CO ₂ insertion		
	R	TS	I	TS2	P
Pd–C3 (Å)	5.323	2.335	2.258	2.397	2.088
Pd–C1 (Å)	2.143	2.183	2.666	2.080	2.088
Pd–O1 (Å)	5.369	2.683	2.666	2.622	2.077
C1–C2 (Å)	1.422	1.406	1.399	1.474	1.535
C2–C3 (Å)	4.249	2.891	2.797	1.836	1.534
C3–O1 (Å)	1.169	1.212	1.224	1.252	1.322
ΔE (kcal/mol)	0.00	6.47	6.32	20.92	–4.75
ΔH (kcal/mol)	0.00	6.07	6.72	20.68	–3.27
ΔG (kcal/mol)	0.00	8.51	8.52	24.43	0.42

Table S7. DFT-computed reaction coordinate of titanalactone formation reaction of compound **1** and CO₂ to generate compound **2**. Protons were omitted for clarity.



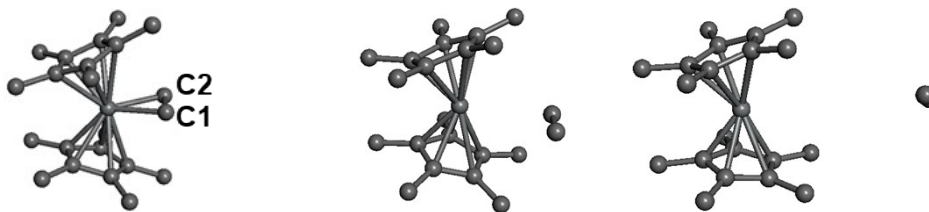
	R	TS	P (2)
Ti–C1 (Å)	2.172	2.197	2.225
Ti–O1 (Å)	5.908	2.551	1.965
C1–C2 (Å)	1.468	1.457	1.537
C2–C3 (Å)	5.534	2.656	1.528
C3–O1 (Å)	1.170	1.185	1.334
C3–O2 (Å)	1.170	1.171	1.228
ΔE (kcal/mol)	0.00	9.62	–24.16
ΔH (kcal/mol)	0.00	9.08	–22.95
ΔG (kcal/mol)	0.00	15.37	–16.30

Table S8. DFT-computed reaction coordinate of ethylene cyclization reaction of compound **1** with additional C₂H₄ to generate compound **4**. Protons were omitted for clarity.



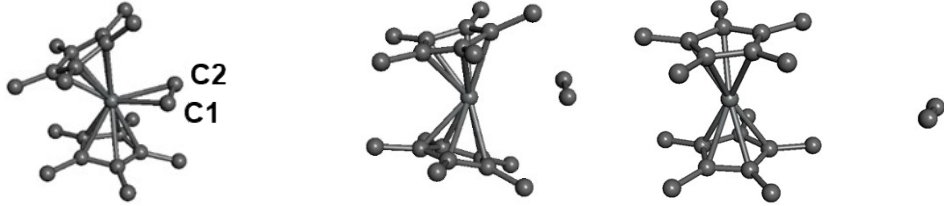
	Ethylene coordination			Ethylene insertion	
	R (1)	TS	P	TS2	P2 (4)
Ti–C1 (Å)	2.171	2.234	2.376	2.223	2.215
Ti–C4 (Å)	6.706	3.255	2.376	2.223	2.229
C1–C2 (Å)	1.468	1.441	1.398	1.457	1.538
C2–C3 (Å)	6.187	2.888	2.485	1.997	1.540
C3–C4 (Å)	1.335	1.344	1.398	1.457	1.551
ΔE (kcal/mol)	0.00	16.18	10.76	15.62	–5.15
ΔH (kcal/mol)	0.00	16.04	11.90	16.30	–4.03
ΔG (kcal/mol)	0.00	24.65	20.89	25.34	4.08

Table S9. DFT-computed reaction coordinate of ethylene dissociation reaction of $S = 0$ state of compound **1**. Protons were omitted for clarity.



	R (1)	TS	P
Ti-C1 (Å)	2.172	3.216	6.023
Ti-C2 (Å)	2.173	3.880	5.993
C1-C2 (Å)	1.468	1.346	1.335
ΔE (kcal/mol)	0.00	35.00	30.58
ΔH (kcal/mol)	0.00	33.75	29.46
ΔG (kcal/mol)	0.00	32.63	19.82

Table S10. DFT-computed reaction coordinate of ethylene dissociation reaction of $S = 1$ state of compound **1**. Energy values were computed relative to the $S = 0$ state of compound **1**. Protons were omitted for clarity.



	R (1)	TS	P
Ti-C1 (Å)	2.412	3.695	6.645
Ti-C2 (Å)	2.412	3.327	1.335
C1-C2 (Å)	1.392	1.343	6.516
ΔE (kcal/mol)	13.36	28.01	20.23
ΔH (kcal/mol)	13.41	27.45	19.82
ΔG (kcal/mol)	12.91	25.18	8.68

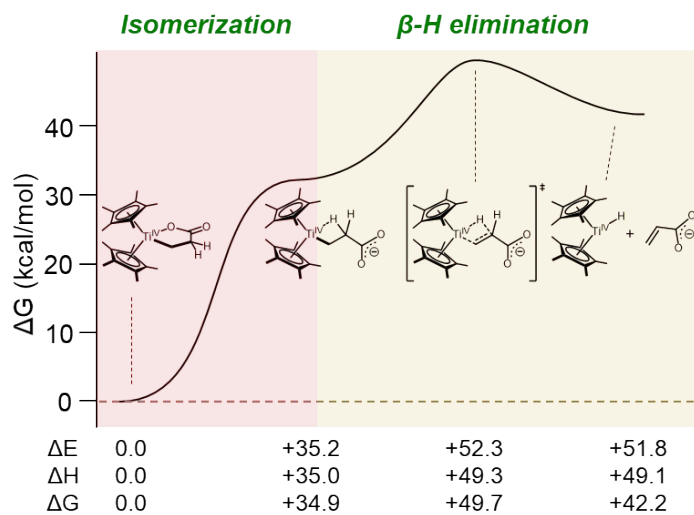
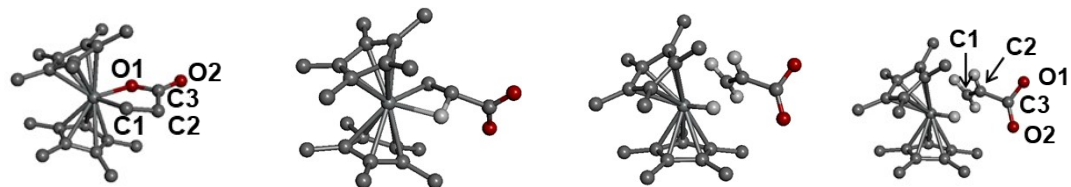


Figure S41. DFT-computed reaction profile of β -hydride elimination pathway of compound **2**.

Table S11. DFT-computed reaction coordinate of β -hydride elimination reaction of compound **2**.



	R (2)	R2	TS	P
Ti–C1 (Å)	2.225	2.143	2.392	2.413
Ti–O1 (Å)	1.965	4.824	4.195	4.206
C1–C2 (Å)	1.537	1.511	1.383	1.378
C2–C3 (Å)	1.528	1.628	1.528	1.526
C3–O1 (Å)	1.334	1.249	1.252	1.253
C3–O2 (Å)	1.228	1.254	1.264	1.264
ΔE (kcal/mol)	0.00	34.38	52.26	52.27
ΔH (kcal/mol)	0.00	33.78	49.25	49.95
ΔG (kcal/mol)	0.00	32.56	49.65	49.20

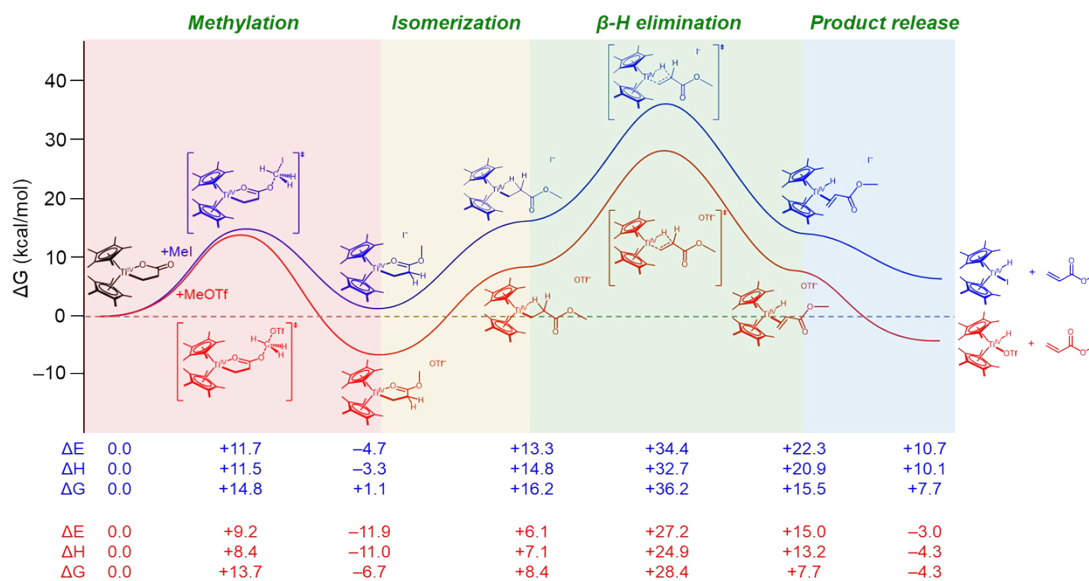
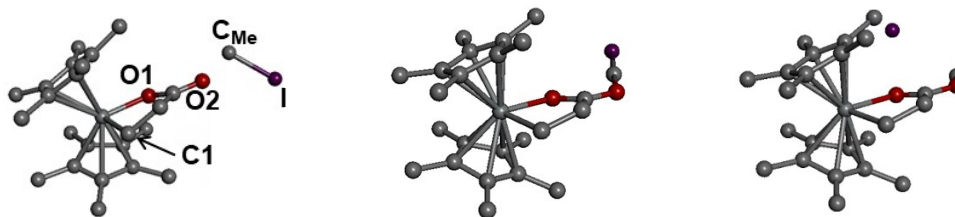


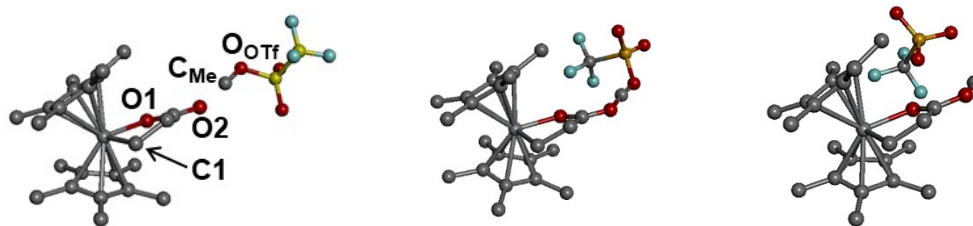
Figure S42. DFT-computed reaction profile of methylation-assisted β -hydride elimination pathway of compound **2**, driven by the addition of MeI (blue) and MeOTf (red).

Table S12. DFT-computed reaction coordinate of methylation of compound **2** with MeI. Protons were omitted for clarity.



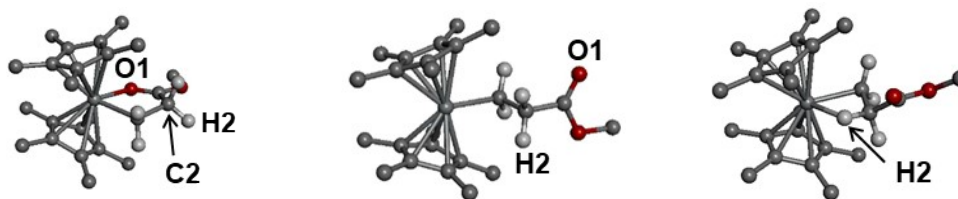
	R (2)	TS	P
Ti-C1 (Å)	2.217	2.223	2.233
Ti-O1 (Å)	1.976	2.026	2.101
O2-C _{Me} (Å)	3.374	2.018	1.474
C _{Me} -I (Å)	2.219	2.698	4.200
ΔE (kcal/mol)	0.00	11.73	-4.68
ΔH (kcal/mol)	0.00	11.48	-3.29
ΔG (kcal/mol)	0.00	14.77	1.14

Table S13. DFT-computed reaction coordinate of methylation of compound **2** with MeOTf to generate compound **5**. Protons were omitted for clarity.



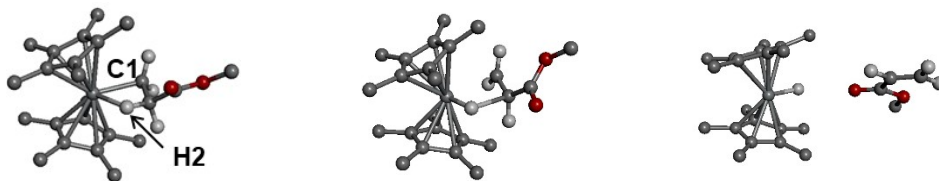
	R (2)	TS	P (5)
Ti–C1 (Å)	2.218	2.223	2.235
Ti–O1 (Å)	1.973	2.023	2.090
O2–C _{Me} (Å)	2.998	2.050	1.476
C _{Me} –O _{OTf} (Å)	1.488	1.896	3.407
ΔE (kcal/mol)	0.00	9.22	–11.94
ΔH (kcal/mol)	0.00	8.43	–11.02
ΔG (kcal/mol)	0.00	13.67	–6.68

Table S14. DFT-computed reaction coordinate of carbonyl dissociation reaction and the formation of Ti–H agostic interaction of compound **5**. Protons other than from ethylene were omitted for clarity.



	R	R2	R3
Ti–C1 (Å)	2.233	2.186	2.159
Ti–O1 (Å)	2.109	5.101	4.377
Ti–H2 (Å)	4.030	3.075	2.091
C2–H2 (Å)	1.098	1.095	1.136
ΔE (kcal/mol)	0.00	18.03	18.78
ΔH (kcal/mol)	0.00	18.12	18.37
ΔG (kcal/mol)	0.00	15.07	16.88

Table S15. DFT-computed reaction coordinate of β -hydride elimination of methylated titanalactone complex $\text{Cp}^*_2\text{Ti}(\text{C}_2\text{H}_4\text{CO}_2\text{Me})$. Protons other than from ethylene were omitted for clarity.



	R	TS	P
Ti-C1 (Å)	2.159	2.487	7.849
Ti-H2 (Å)	4.377	1.709	1.680
C1-C2 (Å)	1.520	1.363	1.340
ΔE (kcal/mol)	0.00	20.32	8.18
ΔH (kcal/mol)	0.00	17.59	5.82
ΔG (kcal/mol)	0.00	18.21	-2.48

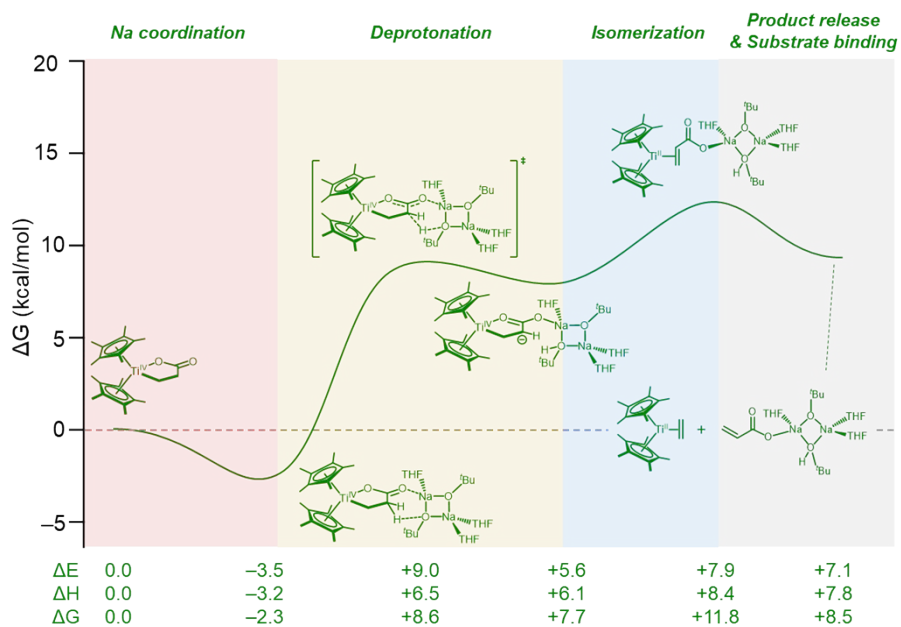
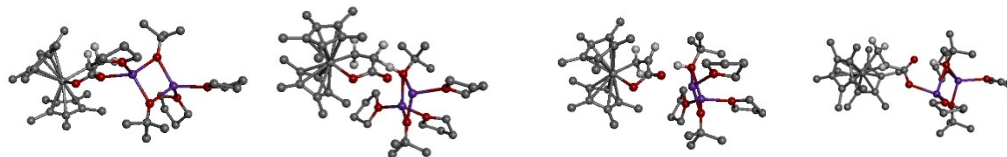


Figure S43. DFT-computed reaction profile of NaO'Bu-assisted deprotonation pathway of compound 2.

Table S16. DFT-computed reaction coordinate of deprotonation of compound **2** assisted by NaO^tBu-THF adduct. Protons other than from ethylene were omitted for clarity.



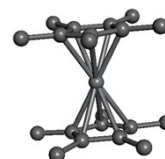
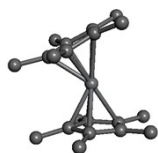
	R	TS	P	P2
Ti–C1 (Å)	2.226	2.197	2.175	2.171
Ti–O1 (Å)	1.984	1.978	2.001	4.054
C1–C2 (Å)	1.539	1.528	1.484	1.466
C2–H2 (Å)	1.099	1.482	2.127	3.801
H2–O_{tBuO} (Å)	3.708	1.208	0.996	1.034
Na–O_{tBuO} (Å)	2.258	2.447	2.558	2.414
ΔE (kcal/mol)	0.0	17.8	13.5	12.5
ΔH (kcal/mol)	0.0	14.6	13.2	12.8
ΔG (kcal/mol)	0.0	19.9	15.2	16.0

Table S17. DFT-computed reaction coordinate of product release and substrate coordination of compound **A**. Protons other than from ethylene molecules were omitted for clarity.



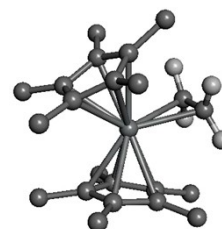
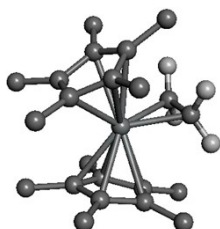
	A + Ethylene	1 + Product
ΔE (kcal/mol)	0.00	–4.94
ΔH (kcal/mol)	0.00	–5.00
ΔG (kcal/mol)	0.00	–4.15

Table S18. Relative energies of the singlet and triplet states of Cp*₂Ti species computed by unrestricted DFT.



	Singlet	Triplet
ΔE (kcal/mol)	+10.49	0
ΔH (kcal/mol)	+11.21	0
ΔG (kcal/mol)	+9.56	0

Table S19. Relative energies of the singlet and triplet states of Compound **1** computed by unrestricted DFT.



	Singlet	Triplet
ΔE (kcal/mol)	0.00	+13.36
ΔH (kcal/mol)	0.00	+13.40
ΔG (kcal/mol)	0.00	+12.91

Table S20. Relative energies of the singlet and triplet states of Intermediate **A** computed by unrestricted DFT.



	Singlet	Triplet
ΔE (kcal/mol)	0.00	+12.12
ΔH (kcal/mol)	0.00	+11.94
ΔG (kcal/mol)	0.00	+9.37

Cartesian coordinates of DFT-optimized structures

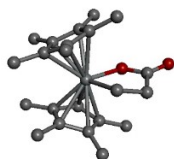
Compound 1



Ti	0.000773	0.353936	-0.106658	C	2.115516	-0.062508	-2.853005
C	0.025813	2.427604	0.541838	H	3.10525	-0.368764	-3.222672
C	-1.62087	-1.29796	0.530331	H	1.373563	-0.707595	-3.336748
C	-1.713382	-1.092142	-0.889877	H	1.937529	0.963376	-3.193756
C	-2.202097	0.235343	-1.109319	C	3.076842	2.161133	-0.76395
C	-2.421511	0.840928	0.165759	H	2.639756	3.007723	-0.219943
C	-2.032705	-0.088866	1.173991	H	4.142039	2.11762	-0.495801
H	-0.838041	2.805866	1.088764	H	3.017672	2.37788	-1.835175
C	-0.053777	2.365888	-0.922956	C	-2.60798	0.798069	-2.446759
C	1.649591	-1.321319	-0.606865	H	-1.897388	0.527258	-3.236138
C	1.740669	-0.995909	0.790741	H	-3.593444	0.40963	-2.746116
C	2.207423	0.353267	0.897156	H	-2.682135	1.890263	-2.420875
C	2.415631	0.853572	-0.424564	C	-1.65041	-2.151734	-1.962478
C	2.040164	-0.163361	-1.350553	H	-2.667683	-2.399231	-2.300711
H	0.807014	2.7031	-1.500685	H	-1.090581	-1.824544	-2.846974
H	-0.990479	2.670675	-1.39111	H	-1.194822	-3.075011	-1.59743
H	0.958903	2.782488	0.981327	C	-1.473464	-2.629934	1.21878
C	1.693501	-1.960334	1.950269	H	-2.460524	-3.109807	1.299807
H	2.714905	-2.171665	2.300453	H	-0.825725	-3.318856	0.668872
H	1.138351	-1.559392	2.807062	H	-1.079114	-2.530636	2.234402
H	1.24092	-2.914819	1.671538	C	-2.117303	0.131274	2.663108
C	2.610888	1.029364	2.181319	H	-3.105735	-0.156003	3.051183

H	1.926137	0.785876	3.001643	H	-1.37108	-0.465342	3.199838
H	3.617335	0.705843	2.488106	H	-1.952713	1.18271	2.922878
H	2.63702	2.118952	2.075696	C	-3.103745	2.161576	0.395131
C	1.523227	-2.708678	-1.180769	H	-2.672659	2.969397	-0.209099
H	2.518334	-3.176601	-1.224187	H	-4.165558	2.08234	0.121957
H	0.888765	-3.360506	-0.572991	H	-3.058027	2.462077	1.446599
H	1.125429	-2.700212	-2.199527				

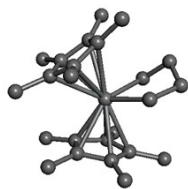
Compound 2



Ti	0.031904	0.445222	-0.034705	H	3.045377	2.483105	-1.362853
C	-1.595749	-1.339917	0.461887	C	-2.86374	1.029058	-2.156651
C	-1.756002	-0.961042	-0.907915	H	-2.368294	0.70303	-3.076786
C	-2.262339	0.382663	-0.938727	H	-3.921776	0.740028	-2.236168
C	-2.359573	0.844191	0.403857	H	-2.825563	2.122121	-2.118615
C	-1.905939	-0.202191	1.268119	C	-1.692546	-1.872363	-2.107408
C	1.672232	-1.336525	-0.444923	H	-2.70723	-2.096151	-2.467013
C	1.664937	-1.072079	0.966654	H	-1.146604	-1.418525	-2.943258
C	2.150596	0.256087	1.162153	H	-1.212237	-2.823834	-1.866047
C	2.462734	0.811969	-0.111949	C	-1.482181	-2.751095	0.971559
C	2.162067	-0.169914	-1.10773	H	-2.487956	-3.196498	0.973487
C	1.523689	-2.085421	2.073974	H	-0.853659	-3.387361	0.343546
H	2.513116	-2.28086	2.511121	H	-1.108303	-2.793788	1.996564
H	0.876993	-1.738726	2.88768	C	-1.917451	-0.127377	2.773196
H	1.13492	-3.037776	1.708451	H	-2.946441	-0.196834	3.154715

C	2.388231	0.925439	2.488106	H	-1.342527	-0.940388	3.227109
H	1.782566	0.475159	3.281262	H	-1.501153	0.823338	3.124657
H	3.444244	0.828104	2.77941	C	-2.978746	2.125353	0.887594
H	2.145386	1.990872	2.438308	H	-3.235889	2.792903	0.059933
C	1.550317	-2.684142	-1.107119	H	-3.90684	1.903845	1.432819
H	2.549342	-3.137316	-1.190883	H	-2.316972	2.664576	1.574974
H	0.929557	-3.38003	-0.53753	C	0.093641	1.926985	-1.693272
H	1.14445	-2.61261	-2.120611	H	1.123955	2.041263	-2.03658
C	2.489595	-0.096302	-2.57579	H	-0.500012	1.653378	-2.573288
H	3.431267	-0.628339	-2.77431	C	-0.36944	3.267871	-1.100609
H	1.71425	-0.561549	-3.194538	C	-0.025805	3.349574	0.386482
H	2.620214	0.93508	-2.916294	H	0.040941	4.150146	-1.611985
C	3.110848	2.151465	-0.322111	H	-1.462682	3.371433	-1.151594
H	2.661541	2.921968	0.314526	O	0.118138	4.395808	1.013883
H	4.177622	2.096026	-0.06255	O	0.071217	2.144392	0.950867

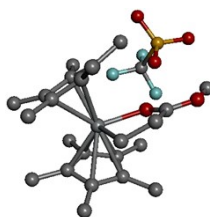
Compound 4



Ti	0.038236	0.468215	-0.021594	H	-2.307568	0.596357	-3.116849
C	-1.610152	-1.311754	0.497783	H	-3.886583	0.684742	-2.327183
C	-1.739021	-0.973772	-0.886571	H	-2.771044	2.055614	-2.226991
C	-2.263346	0.356343	-0.968293	C	-1.665668	-1.920205	-2.058688
C	-2.422168	0.850604	0.358423	H	-2.677049	-2.127461	-2.43814
C	-1.974896	-0.165046	1.262966	H	-1.088153	-1.507051	-2.894678
C	1.651977	-1.31288	-0.499702	H	-1.218495	-2.877278	-1.78018

C	1.672223	-1.110692	0.920913	C	-1.492983	-2.707005	1.051339
C	2.208833	0.186644	1.169648	H	-2.493581	-3.165139	1.053686
C	2.514388	0.793115	-0.083286	H	-0.847429	-3.356188	0.453634
C	2.163976	-0.131675	-1.116486	H	-1.132472	-2.716437	2.08249
C	1.54148	-2.162685	1.993221	C	-2.074037	-0.088162	2.764383
H	2.536924	-2.381478	2.407685	H	-3.086723	-0.355952	3.101587
H	0.913251	-1.839135	2.831323	H	-1.373858	-0.771957	3.256214
H	1.137951	-3.099796	1.604784	H	-1.867224	0.924796	3.12757
C	2.586867	0.691921	2.536808	C	-3.195067	2.077122	0.766016
H	1.771048	0.581853	3.260888	H	-3.507179	2.661576	-0.10496
H	3.442991	0.11664	2.919986	H	-4.10497	1.773704	1.303417
H	2.882898	1.744901	2.517189	H	-2.633274	2.740799	1.435039
C	1.498473	-2.634239	-1.207032	C	0.074848	2.326107	1.210243
H	2.481758	-3.12339	-1.278715	H	-0.830424	2.354889	1.830254
H	0.835732	-3.322882	-0.676269	H	0.915574	2.358246	1.912655
H	1.122033	-2.517596	-2.227471	C	0.073815	1.979196	-1.641421
C	2.479432	0.008779	-2.582485	H	1.116285	2.185471	-1.912659
H	3.453305	-0.452454	-2.804639	H	-0.427839	1.66146	-2.567236
H	1.732342	-0.485941	-3.213054	C	-0.526919	3.280248	-1.077453
H	2.537588	1.057589	-2.889295	C	0.127458	3.568945	0.284485
C	3.260273	2.085119	-0.270184	H	-0.330346	4.454317	0.760074
H	3.082441	2.779358	0.557383	H	1.177812	3.83391	0.101137
H	4.342313	1.891024	-0.313001	H	-0.376487	4.133054	-1.766025
H	2.98422	2.590878	-1.201775	H	-1.611303	3.187673	-0.946434
C	-2.826887	0.96273	-2.225162				

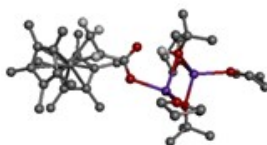
Compound 5



Ti	0.007339	0.848678	0.46914	H	-2.248187	-2.823662	-0.722481
C	-1.431748	-0.742931	1.585629	H	-0.66544	-2.372863	-1.356943
C	-1.469679	-1.059453	0.184423	H	-0.802403	-3.120016	0.247987
C	-2.082019	0.036855	-0.497644	C	-1.161752	-1.693496	2.721842
C	-2.425381	1.028207	0.472083	H	-2.10631	-2.176991	3.010633
C	-2.022782	0.54508	1.756732	H	-0.462482	-2.488389	2.452675
C	1.778362	-0.846623	0.541993	H	-0.778569	-1.177007	3.606332
C	1.923427	0.026893	1.665777	C	-2.275962	1.209662	3.083222
C	2.27824	1.324921	1.169559	H	-3.055704	0.658319	3.627295
C	2.315368	1.263171	-0.253679	H	-1.38335	1.235456	3.715797
C	1.95509	-0.069973	-0.644041	H	-2.624346	2.237507	2.953691
C	1.98741	-0.364968	3.119298	C	-3.211708	2.284862	0.22328
H	3.038798	-0.394131	3.440302	H	-3.074686	2.665965	-0.793517
H	1.475163	0.356879	3.763615	H	-4.283837	2.082528	0.352693
H	1.565252	-1.35725	3.294486	H	-2.948054	3.079597	0.928681
C	2.713443	2.47465	2.036587	C	-0.225226	2.280159	-1.231942
H	2.129195	2.527871	2.960742	H	0.447722	2.056749	-2.066613
H	3.768211	2.338157	2.315349	H	-1.238896	2.228984	-1.632628
H	2.63937	3.435426	1.51658	C	0.024785	3.7128	-0.714148
C	1.801123	-2.349518	0.595979	C	-0.154835	3.751106	0.776708
H	2.848089	-2.666052	0.708682	H	1.054846	4.045898	-0.899396
H	1.250969	-2.759378	1.446327	H	-0.618262	4.477021	-1.169969
H	1.422696	-2.805656	-0.320969	O	-0.252511	4.932984	1.341365

C	1.982167	-0.586769	-2.058094	O	-0.179329	2.688488	1.442694
H	3.016377	-0.804492	-2.36109	O	0.60252	3.591879	7.153959
H	1.406701	-1.51074	-2.166969	S	1.010687	2.422675	6.333332
H	1.582744	0.148874	-2.764754	O	2.376131	1.896712	6.591998
C	2.946414	2.274317	-1.171534	O	0.632737	2.507932	4.891865
H	3.073755	3.246579	-0.686957	C	-0.110721	1.040976	6.966657
H	3.947713	1.916852	-1.449527	F	0.145485	-0.1324	6.331897
H	2.389503	2.415622	-2.104655	F	-1.417667	1.339118	6.761969
C	-2.467267	0.018206	-1.952792	F	0.06285	0.835227	8.292601
H	-1.64334	-0.312155	-2.594682	C	-0.395344	5.000425	2.809211
H	-3.299663	-0.684674	-2.099907	H	-0.044692	5.998343	3.066699
H	-2.803515	0.998329	-2.302572	H	-1.45537	4.888446	3.045877
C	-1.267128	-2.414306	-0.442667	H	0.194254	4.217971	3.288101

Compound A



Ti	-0.111951	0.240328	-0.156555	C	-1.059463	7.800644	4.956852
C	0.006698	-2.092301	0.558311	C	-1.510734	5.473074	5.191542
C	-1.369342	-1.836746	0.267152	C	-1.960064	7.603346	6.176603
C	-1.857923	-0.899276	1.224162	H	-0.034516	8.065406	5.253289
C	-0.770855	-0.519172	2.069118	H	-1.429592	8.544779	4.24491
C	0.386845	-1.253039	1.659162	C	-1.642653	6.146462	6.561846
C	1.35672	-0.361122	-1.932041	H	-2.478162	5.108777	4.821632
C	2.182917	0.128107	-0.860607	H	-0.788808	4.650055	5.176029
C	1.898122	1.518967	-0.69154	H	-3.014921	7.703649	5.893741
C	0.948251	1.900817	-1.683694	H	-1.742602	8.317724	6.97652

C	0.584463	0.738173	-2.426439	H	-2.419314	5.683068	7.177665
C	3.371862	-0.580374	-0.265783	H	-0.691796	6.098451	7.105769
H	4.255706	-0.402585	-0.89686	O	0.352625	7.391783	-2.828512
H	3.61177	-0.21528	0.73713	C	-0.671404	7.2386	-3.85577
H	3.230926	-1.663028	-0.207857	C	1.673359	7.22431	-3.429969
C	2.545394	2.451225	0.301708	C	0.066228	7.360565	-5.190021
H	2.996261	1.898042	1.133152	H	-1.139709	6.251253	-3.742999
H	3.345524	3.038084	-0.173412	H	-1.425924	8.014995	-3.694295
H	1.810951	3.150501	0.716813	C	1.42423	6.717962	-4.853789
C	1.515556	-1.66701	-2.671158	H	2.17805	8.199801	-3.430206
H	2.036872	-1.487127	-3.623291	H	2.243257	6.525983	-2.809363
H	2.109588	-2.388946	-2.106516	H	0.198439	8.415624	-5.458972
H	0.555244	-2.135445	-2.918279	H	-0.460494	6.855089	-6.005176
C	-0.273643	0.713316	-3.663842	H	2.222752	7.009893	-5.542589
H	0.344354	0.835766	-4.566962	H	1.337996	5.625118	-4.862784
H	-0.81572	-0.233697	-3.764967	C	2.468179	7.933315	1.600888
H	-1.00899	1.52445	-3.655861	C	-3.346133	7.011958	0.370434
C	0.602859	3.309199	-2.0708	C	3.00197	6.896263	2.628798
H	-0.460013	3.444965	-2.287262	H	2.349472	6.877521	3.512815
H	0.867602	4.020593	-1.284902	H	2.999063	5.893246	2.180787
H	1.175895	3.572942	-2.973428	H	4.025741	7.120658	2.964101
C	-3.298422	-0.513713	1.424595	C	2.494596	9.337674	2.266903
H	-3.932121	-0.901024	0.620664	H	1.822034	9.348092	3.135021
H	-3.667771	-0.936891	2.3692	H	3.500432	9.629678	2.605339
H	-3.442293	0.573419	1.476146	H	2.139237	10.091236	1.551304
C	-2.192785	-2.516459	-0.797312	C	3.431862	7.95273	0.382384
H	-2.720896	-3.392741	-0.39329	H	3.438469	6.965128	-0.097845
H	-2.946714	-1.838019	-1.211996	H	3.079654	8.687816	-0.354462

H	-1.567686	-2.865904	-1.625999	H	4.465318	8.210035	0.659673
C	0.779626	-3.28614	0.061644	C	-3.931264	6.134021	1.492742
H	0.596978	-4.135853	0.736726	H	-3.814002	5.074557	1.23888
H	0.466229	-3.59607	-0.938829	H	-3.407461	6.328022	2.436252
H	1.860114	-3.118284	0.044025	C	-4.061851	6.729333	-0.96309
C	1.649386	-1.352818	2.47923	H	-5.135416	6.944331	-0.886565
H	1.442432	-1.890151	3.41688	H	-3.638098	7.353556	-1.759206
H	2.43577	-1.901003	1.955296	H	-3.934258	5.676376	-1.238803
H	2.047496	-0.369153	2.755593	H	-4.999052	6.343627	1.63611
C	-0.858164	0.322947	3.316095	C	-3.446696	8.496978	0.73852
H	-1.73944	0.973525	3.306832	H	-2.876615	8.701986	1.652675
H	-0.935194	-0.319853	4.206156	H	-3.048459	9.122107	-0.069471
H	0.025474	0.958132	3.44539	H	-4.492049	8.780893	0.909977
C	-1.920136	1.270323	-0.776206	O	-0.286032	10.459691	-1.021411
H	-1.880637	1.836027	-1.707356	C	-0.744655	11.46586	-0.071988
H	-2.858398	0.718658	-0.678458	C	0.463636	11.112503	-2.092646
C	-1.377213	1.972192	0.390292	C	0.125935	12.695103	-0.331413
C	-1.174795	3.456256	0.47914	H	-1.805798	11.680843	-0.263034
H	-1.834325	5.721437	-0.041344	H	-0.637707	11.046304	0.932724
H	-1.760842	1.656231	1.359072	C	0.314818	12.620121	-1.857675
O	-0.539726	3.914842	1.493546	H	1.510782	10.790967	-2.019395
O	-1.713869	4.213039	-0.412614	H	0.053661	10.77989	-3.051955
Na	-0.281486	6.125306	2.037352	H	1.090427	12.595759	0.180963
Na	-0.103043	8.080942	-0.573866	H	-0.351985	13.622831	-0.001979
O	-1.929258	6.717008	0.220424	H	1.184079	13.181466	-2.213327
O	1.173185	7.606796	1.196733	H	-0.577653	13.002166	-2.367387
O	-1.037276	6.511286	4.279357				

XIV. Reference

- 1 T. T. Nguyen, G. D. Kortman and K. L. Hull, *Organometallics*, 2016, **35**, 1713–1725.
- 2 M. Kessler, S. Hansen, D. Hollmann, M. Klahn, T. Beweries, A. Spannenberg, A. Brückner and U. Rosenthal, *Eur. J. Inorg. Chem*, 2011, **2011**, 627–631.
- 3 D. F. Evans, *J. Chem. Soc.*, 1959, 2003.
- 4 S. Stoll and A. Schweiger, *J. Magn. Reson.*, 2006, **178**, 42–55.
- 5 S. A. Cohen, P. R. Auburn and J. E. Bercaw, *J. Am. Chem. Soc.*, 1983, **105**, 1136–1143.
- 6 S. A. Cohen and J. E. Bercaw, *Organometallics*, 1985, **4**, 1006–1014.
- 7 M. Penhoat, *Tetrahedron Letters*, 2013, **54**, 2571–2574.
- 8 S. Tshepelevitsh, A. Kütt, M. Lökov, I. Kaljurand, J. Saame, A. Heering, P. G. Plieger, R. Vianello and I. Leito, *Eur. J. Org. Chem.*, 2019, **2019**, 6735–6748.
- 9 P. B. Kisanga, J. G. Verkade and R. Schwesinger, *J. Org. Chem.*, 2000, **65**, 5431–5432.
- 10 W. N. Olmstead, Z. Margolin and F. G. Bordwell, *J. Org. Chem.*, 1980, **45**, 3295–3299.
- 11 C. R. Waidmann, A. J. M. Miller, C.-W. A. Ng, M. L. Scheuermann, T. R. Porter, T. A. Tronic and J. M. Mayer, *Energy Environ. Sci.*, 2012, **5**, 7771.
- 12 J. W. Shin, K. Eom and D. Moon, *J. Synchrotron Rad.*, 2016, **23**, 369–373.
- 13 Z. Otwinowski and W. Minor, in *Methods in Enzymology*, Elsevier, 1997, vol. 276, pp. 307–326.
- 14 G. M. Sheldrick, *Acta Crystallogr. C. Struct. Chem.*, 2015, **71**, 3–8.
- 15 M. J. Frisch, G. W. Trucks, H. B. Schlegel, G. E. Scuseria, M. A. Robb, J. R. Cheeseman, G. Scalmani, V. Barone, G. A. Petersson, H. Nakatsuji, X. Li, M. Caricato, A. V. Marenich, J. Bloino, B. G. Janesko, R. Gomperts, B. Mennucci, H. P. Hratchian, J. V. Ortiz, A. F. Izmaylov, J. L. Sonnenberg, D. Williams-Young, F. Ding, F. Lipparini, F. Egidi, J. Goings, B. Peng, A. Petrone, T. Henderson, D. Ranasinghe, V. G. Zakrzewski, J. Gao, N. Rega, G. Zheng, W. Liang, M. Hada, M. Ehara, K. Toyota, R. Fukuda, J. Hasegawa, M. Ishida, T. Nakajima, Y. Honda, O. Kitao, H. Nakai, T. Vreven, K. Throssell, J. A. Montgomery, Jr., J. E. Peralta, F. Ogliaro, M. J. Bearpark, J. J. Heyd, E. N. Brothers, K. N. Kudin, V. N. Staroverov, T. A. Keith, R. Kobayashi, J. Normand, K. Raghavachari, A. P. Rendell, J. C. Burant, S. S. Iyengar, J. Tomasi, M. Cossi, J. M. Millam, M. Klene, C. Adamo, R. Cammi, J. W. Ochterski, R. L. Martin, K. Morokuma, O. Farkas, J. B. Foresman, and D. J. Fox, Gaussian 16 (version Revision C.01) Gaussian, Inc., Wallingford, CT 2016.
- 16 J. Tao, J. P. Perdew, V. N. Staroverov and G. E. Scuseria, *Phys. Rev. Lett.*, 2003, **91**, 146401.
- 17 R. Krishnan, J. S. Binkley, R. Seeger and J. A. Pople, *J. Chem. Phys.*, 1980, **72**, 650–654.
- 18 A. D. McLean and G. S. Chandler, *J. Chem. Phys.*, 1980, **72**, 5639–5648.
- 19 M. M. Francl, W. J. Pietro, W. J. Hehre, J. S. Binkley, M. S. Gordon, D. J. DeFrees and J. A. Pople, *J. Chem. Phys.*, 1982, **77**, 3654–3665.
- 20 V. Barone and M. Cossi, *J. Phys. Chem. A*, 1998, **102**, 1995–2001.